

**Dissertation zur Erlangung des Doktorgrades
der Fakultät für Biologie
der Ludwig-Maximilians-Universität München**

Proliferation and arrest of human tetraploid cells

Christian Kuffer

aus

München

2015

Eidesstattliche Erklärung

Hiermit erkläre ich, dass ich die vorliegende Dissertation selbstständig und ohne unerlaubte Hilfe angefertigt habe. Ich habe weder anderweitig versucht, eine Dissertation einzureichen oder eine Doktorprüfung durchzuführen, noch habe ich diese Dissertation oder Teile derselben einer anderen Prüfungskommission vorgelegt.

München, den 20. Januar 2015

Christian Kuffer

1. Gutachter: Prof. Dr. Stefan Jentsch
2. Gutachter: Prof. Dr. Angelika Böttger

Promotionsgesuch eingereicht am 20. Januar 2015

Mündliche Prüfung (Disputation) am 24. April 2015

Die vorliegende Arbeit wurde zwischen Februar 2008 und Juli 2013 unter der Anleitung von Zuzana Storchová (Ph.D.) am Max-Planck-Institut für Biochemie in Martinsried durchgeführt.

Wesentliche Teile dieser Arbeit wurden in den folgenden Publikationen veröffentlicht:

Erstautorenschaft:

Kuffer C, Kuznetsova, A.Y., and Storchova, Z. (2013). Abnormal mitosis triggers p53-dependent cell cycle arrest in human tetraploid cells. *Chromosoma* 122(4):305-18.

Ko-Autorenschaften:

Storchova Z, Kuffer C, (2008). The consequences of tetraploidy and aneuploidy. *J. Cell Sci.* 121: 3859-3866.

Shaposhnikov, D., Kuffer, C., Storchova, Z., and Posern, G. (2013). Myocardin related transcription factors are required for coordinated cell cycle progression. *Cell Cycle* 12, 1762–1772.

Declaration of contribution

Christian Kuffer contributed to the publication

Shaposhnikov, D., Kuffer, C., Storchova, Z., and Posern, G. (2013). Myocardin related transcription factors are required for coordinated cell cycle progression. *Cell Cycle* 12, 1762–1772.

by carrying out all flow cytometric cell sorting experiments to generate the stable cell lines NIH:3T3 H2B-GFP and NIH:3T3 FUCCI used to generate the data presented in the figures 3 and 5 and discussed all the results.

Martinsried, den 16. Januar 2015

Dr. Zuzana Stochová

I. TABLE OF CONTENTS

1. INTRODUCTION	1
1.1 The cell cycle and its control	2
1.1.1 The G ₁ /S checkpoint	4
1.1.2 The DNA-damage checkpoint	7
1.1.3 The G ₂ /M checkpoint	8
1.1.4 The spindle assembly checkpoint	10
1.2 The links between tumorigenesis and tetraploidization	13
1.2.1 Aberrant tetraploidization	14
1.2.2 Tetraploidy-driven tumorigenesis	15
1.2.1 Mechanisms preventing cell proliferation after tetraploidization	18
2. RESULTS	21
2.1 Abnormal mitosis triggers p53-dependent cell cycle arrest in human tetraploid cells	21
2.2 Myocardin related transcription factors are required for coordinated cell cycle progression	22
2.3 A genome-wide screen identifies genes enhancing, as well as restricting, cellular proliferation after tetraploidization.	23
2.3.1 Experimental Setup	23
2.3.2 Primary screen	25
2.3.3 Selection of primary hits	28
2.3.4 Effective reproducibility between the duplicate runs of the primary screen	31
2.3.5 The impact of the SSMD of TP53 controls on the number of primary hits	32
2.3.6 The confirmatory screen of primary TP53-like hits endorses the quality of the primary screen	35
2.3.7 The pathway analysis of the confirmed TP53-like hits	38
2.3.8 Canonical Wnt signaling might support the proliferation after tetraploidization	40
2.3.9 Meta-analysis of the 'Project Achilles' and the identified primary KIFC1-like hits reveal common vulnerabilities of cells CIN	42
3. DISCUSSION	46
3.1 ROS trigger a p53-mediated arrest due to chromosome segregation errors after tetraploidization	47

I. TABLE OF CONTENTS

3.2	The effect of Myocardin-related transcription factors A and B on the proliferation tetraploid and chromosomally unstable cells	50
3.3	Genome-wide screen for genes that modulate the cell proliferation after tetraploidization	52
3.3.1	Setup and quality	52
3.3.2	The TP53-like hit and ATM target CCDC6 might contribute to the arrest after tetraploidization via the activation of 14-3-3 σ	54
3.3.3	Do decreased levels of the DNA polymerase α -primase complex increase the cell proliferation after tetraploidization?	55
3.3.4	Wnt signaling activation enhances the proliferation after tetraploidization	57
3.3.5	Identifying novel anti-cancer drug targets using a meta-analysis of the 'Project Achilles' and the primary KIFC1-like hits	58
3.4	Future directions	60
4.	MATERIAL & METHODS OF UNPUBLISHED DATA	61
4.1.1	HCT116 Fucci	61
4.1.2	Experimental procedures of the primary and confirmatory screen	61
4.1.3	Data evaluation and hit selection for the primary screen	62
4.1.4	Statistical analysis of the confirmatory screen and evaluation of biological pathways	63
4.1.5	Meta-analysis of KIFC1-like primary hits and 'Project Achilles'	63
4.1.6	Data processing and visualization	64
5.	REFERENCES	65

II. ABBREVIATIONS

8-OHdG	8-Hydroxy-Guanosine
APC	Adenomatous-polyposis-coli-Protein
APC/C	Anaphase promoting complex / cyclosome
ATM	Ataxia telangiectasia mutated
ATR	Ataxia telangiectasia and Rad3-related protein
Bub1	Budding uninhibited by benzimidazoles 1
BubR1	Budding uninhibited by benzimidazoles related 1
CCDC6	Coiled-coil domain-containing protein 6
Cdk	Cyclin-dependent kinases
Chk1/2	Checkpoint kinase 1/2
CIN	Chromosomal instability
DNA	Deoxyribonucleic Acid
EGFR	Epidermal growth factor receptor
Erk	Extracellular signal-regulated kinases
FAP	Familial adenomatous polyposis
FDA	Food and Drug Administration
FGFR	Fibroblast growth factor receptor
FUCCI	Fluorescent Ubiquitination-based Cell Cycle Indicator
GSK-3	Glycogen synthase kinase 3
HGFR	Hepatocyte growth factor receptor
hTERT RPE-1	hTERT-immortalized human retina epithelia cells
JAK	Janus kinase
KIFC1-like hit	gene identified to repressed the proliferation of tetraploid cells upon esiRNA knockdown

II. ABBREVIATIONS

MCC	Mitotic checkpoint complex
MAPK	Mitogen-Activated Protein Kinase
MAPKK	MAPK kinase
MAPKKK (RAF)	MAPKK kinase (Rapidly Accelerated Fibrosarcoma)
MEF	Mouse embryonic fibroblast
MRTFs	Myocardin related transcription factors
Nrf2	Nuclear factor-erythroid 2-related factor 2
RNA	Ribonucleic Acid
RNAi	RNA interference
ROS	Reactive Oxygen Species
SAC	Spindle Assembly Checkpoint
ssDNA	single stranded-DNA
STAT	Signal Transducer and Activator of Transcription
TP53-like hit	gene identified to enhance the proliferation of tetraploid cells upon esiRNA knockdown

III. ZUSAMMENFASSUNG

Durch Fehler entstandene tetraploide Zellen sind chromosomal instabil und können zu Zelltransformation führen. Die Beweise verdichten sich, dass die Propagation von tetraploiden Säugetierzellen durch einen p53-vermittelten Arrest eingeschränkt wird; jedoch ist weiterhin unklar, was die Ursache dieses p53-vermittelten Arrests ist.

Um die Ursache des p53-vermittelten Arrests zu identifizieren, wurden individuelle Zellen mittels zeitraffender Mikroskopie in Echtzeit verfolgt. Neu entstandene tetraploide Zellen können einen Zellzyklus vollenden, aber die Mehrzahl der Zellen starb oder verharrte in einem Arrest in der folgenden G1-Phase, abhängig davon ob die vorangegangene Mitose fehlerfrei verlief oder nicht. Tochterzellen, denen eine fehlerhafte Mitose voranging, akkumulierten p53 im Zellkern, was zum Zelltod oder einem irreversiblen Zellzyklusarrest führte. Es zeigte sich durch den Anstieg von 8-OHdG, einem Indikator für oxidative DNA Schädigung, dass tetraploide Zellen durch die vermehrten fehlerhaften Mitosen höheren Konzentrationen von reaktiven oxidativen Spezies (ROS) ausgesetzt sind. Der Anstieg von 8-OHdG korrelierte mit der p53-Akkumulation im Zellkern. Da keine vermehrte Phosphorylierung des Histons H2AX (γ -H2AX), ein Marker für DNA-Strangbrüche, detektiert wurde, lässt sich schlussfolgern, dass ROS entscheidend für den p53 vermittelten Arrest verantwortlich sind.

Mehrere p53-aktivierende Kinasen wurden mittels RNA Interferenz (RNAi) und chemischer Genetik untersucht, ob sie einen Einfluss auf den Zellzyklusarrest von tetraploiden Zellen haben. Von den getesteten Kinasen hatte nur ATM einen Einfluss auf die Aktivierung von p53 nach fehlerhaften tetraploiden Mitosen. Zwar wird ATM in der Regel durch DNA-Schäden aktiviert, jedoch wurde bereits zuvor gezeigt, dass ATM auch durch erhöhte ROS Konzentrationen aktiviert werden kann.

III. ZUSAMMENFASSUNG

Um die Zusammenhänge des Zellzyklusarrests weiter aufzuklären, wurde ein genomübergreifender esiRNA Screen etabliert, der die Zellproliferation nach induzierter Tetraploidisierung analysiert. Durch Kombination der Zellzyklusanalyse anhand des DNA-Gehalts zusammen mit den FUCCI-Zellzyklusindikatoren, konnten tetraploide und diploide Zellen nebeneinander mikroskopisch analysiert werden, ohne zuvor tetraploide und diploide Zellen isolieren zu müssen. Dieser neue experimentelle Ansatz ermöglichte die Identifikation von Genen, die spezifisch die Proliferation von tetraploiden Zellen verstärken oder einschränken

Im Primärscreen wurden 1159 Gene identifiziert, deren Inhibition die Proliferation einschränken. Weiter wurden 431 Gene identifiziert, deren Inhibition die Proliferation der tetraploiden Zellen verstärken. Von den 431 Genen, deren Inhibition die Proliferation verstärken, wurden 371 Gene einem Konfirmationsscreen unterzogen, in dem 158 der identifizierten 371 Gene bestätigt wurden. Die bioinformatische Analyse der 158 Gene zeigte eine signifikante Anhäufung von Genen, die mit DNA-Replikation, dem kanonischen Wnt-Signalweg oder mit Tumorsignalwegen assoziiert sind. Unter letzteren ist CCDC6 sehr interessant, da dessen Genprodukt durch ATM phosphoryliert wird und nachgeschaltet den Tumorsuppressor 14-3-3 σ reguliert.

Des Weiteren wurden mittels einer Meta Analyse der Ergebnisse des Primärscreens, zusammen mit den Daten aus dem "Project Achilles", welches genomweit den Effekt von shRNA-vermittelter Geninhibition auf die Proliferation von 108 Krebszelllinien untersuchte, 18 Gene identifiziert, deren Inhibition sowohl die Proliferation von tetraploiden Zellen einschränkt, als auch die Proliferation von Zelllinien hemmt, welche von Krebsarten stammen, die zu meist chromosomale Instabilitäten (CIN) aufweisen.

Damit bilden die präsentierten Daten nicht nur eine gute Basis zur Aufklärung des Zellzyklusarrests tetraploider Zellen, sondern auch für die Identifikation neuer

III. ZUSAMMENFASSUNG

potentieller Zielmoleküle, welche benutzt werden können um Tumorerkrankungen mit chromosomaler Instabilität zu behandeln, welche häufig resistent gegen die bislang verfügbaren Behandlungen sind.

IV. SUMMARY

Erroneously arising tetraploid mammalian cells are chromosomally unstable and may facilitate cell transformation. An increasing body of evidence suggests that the propagation of mammalian tetraploid cells is limited by a p53-dependent arrest, however, the triggers of this arrest have thus far not been identified.

To elucidate the timing and causes of this arrest, time-lapse live cell imaging was performed to track the fate of individual cells immediately after tetraploidization. Newly formed tetraploid cells can progress through one cell cycle, but the majority of cells arrest or die in the subsequent G1 stage, with the fate of these tetraploid cells determined by the preceding mitosis. Daughter cells arising from defective mitosis accumulated p53 in the nucleus, which led to irreversible cell cycle arrest or death. Furthermore this p53 accumulation coincides and correlates with an increase of the oxidative DNA damage marker 8-OHdG, suggesting an increase in reactive oxygen species (ROS), but does not coincide with the phosphorylation of H2AX (γ -H2AX), a marker for canonical DNA damage.

Using RNA interference and chemical genetics, several p53 activating kinases were tested for their contribution to the cell cycle arrest of tetraploid cells. Of the tested kinases, only ATM was shown to play a role in the activation of p53 after defects in mitosis. ATM kinase is a DNA damage-responsive kinase, however, it has been shown that increased ROS levels activate ATM in a non-canonical way.

To gain further insights into arrest of tetraploid cells, an unbiased genome-wide esiRNA screen was performed to analyze cell proliferation after induced tetraploidization. Using FUCCI cell cycle probes, combined with DNA content cell cycle profiling, allowed an image-based assay to examine tetraploid and diploid cells side-by-side. This novel approach enabled us to screen for genes that specifically

IV. SUMMARY

restricts or enhances cell proliferation after tetraploidization, if inhibited by esiRNA mediated knockdown.

From the primary screen we identified 1159 genes that decreased and 431 genes that increased the cell proliferation after tetraploidization, if knocked down by esiRNA. From the 431 genes that increased proliferation upon knockdown, 374 were selected and subjected to a re-screen. Of these 374 genes, we were able to confirm the results for 158 of the genes. A bioinformatics analysis of the 158 genes for which the phenotype were confirmed by the re-screen revealed a significant enrichment of genes involved in DNA replication, the canonical Wnt signaling pathway and in pathways linked to cancer. Among the latter, CCDC6 is particularly interesting, because its gene product is a target of the ATM kinase and an upstream regulator of the tumor suppressor 14-3-3 σ .

Moreover, by comparing the results of the primary screen with the data of the “Project Achilles”, which measured the proliferation in genome wide pooled-shRNA screens for 108 cancer cell lines, 18 genes were identified that are essential for the proliferation of cells after tetraploidization, as well as for the proliferation of cancer cell lines that derive from cancer types with a high incidence for chromosomal instability (CIN).

Taken together, the presented data builds an excellent resource not only for elucidating how the arrest after tetraploidization is mediated, but also to identify novel potential therapeutic targets against tumors with CIN, which are frequently resistant to many of today’s anti-cancer therapies.

1. INTRODUCTION

The doubling of diploid genomes, called tetraploidization, is a common phenomenon. Two tetraploidizations occurring rapidly after the divergence of cephalochordates but before the split of teleosts and tetrapods fueled the evolution of modern vertebrates including mammals and humans (Ohno, 1970; Dehal and Boore, 2005; Kasahara, 2007; Putnam et al., 2008) and tetraploidization also occurs during the development of several human tissues (Davoli and de Lange, 2011; Lee et al., 2009).

However, several observations raised the hypothesis that tumorigenesis could be promoted, or eventually even initiated, by un-scheduled tetraploidization followed by chromosome loss and structural rearrangements of chromosomes, known as numerical and structural chromosomal instability (CIN) (Shackney et al., 1989; Storchova and Pellman, 2004; Ganem et al., 2007). Therefore, scientists have begun to investigate whether cells stop proliferating after un-scheduled tetraploidization, and if tetraploidization itself is sufficient to trigger tumorigenesis. Chapter 1.2. reviews the current body of evidence suggesting that tetraploidization contributes to tumorigenesis, and presents possible mechanisms by which cells prevent proliferation after un-scheduled tetraploidization.

Uncontrolled proliferation is a hallmark of cancer cells (Vermeulen et al., 2003); thus, in the following chapter (1.1) I will describe the molecular mechanisms that regulate cell cycle progression, thereby preventing uncontrolled cell proliferation and ensuring error-free propagation of genetic information during cell proliferation. Moreover, the molecular mechanisms controlling cell cycle progression are also the starting point for investigating the proliferation of cells after unscheduled tetraploidization.

1. INTRODUCTION

1.1 The cell cycle and its control

To divide genetic information equally into two daughter cells during mitosis, the cells must first double their chromosomes in S-phase. During the cell cycle, mitosis or M-phase and S-phase are preceded by the gap or growth phases G_1 and G_2 , in which cells prepare for the S- or M-phase, respectively.

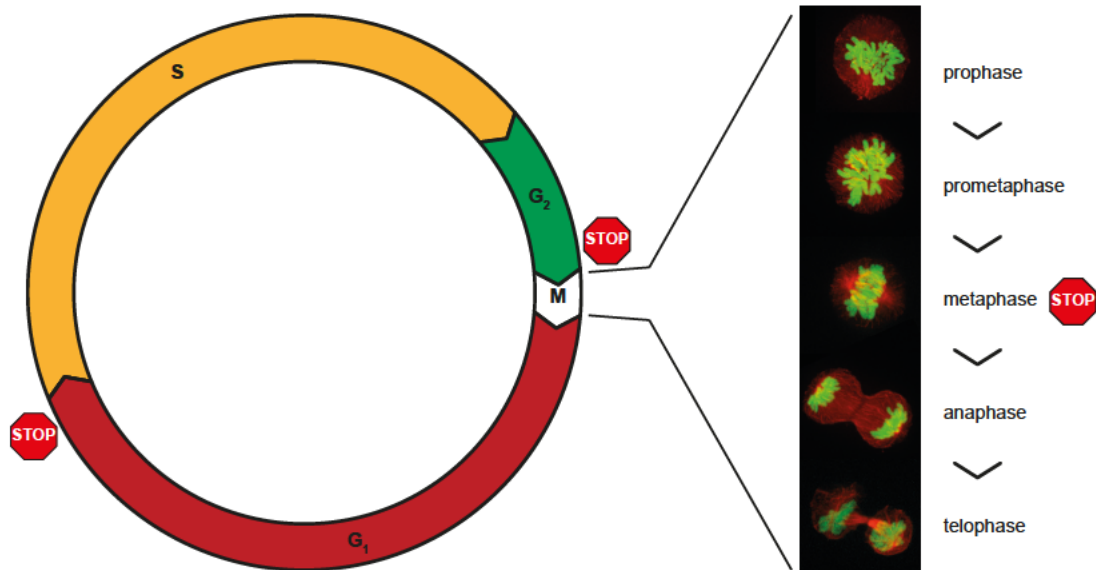


Figure 1: The cell cycle and its checkpoints

The circle depicts a simplified representation of the cell cycle and its checkpoints. G_1 -phase is represented in red, S-phase in orange, G_2 -phase in green and M-phase/mitosis in white. The stop signs indicate the checkpoints at G_1/S and G_2/M transition. On the right, the micrographs show the mitotic progression and the stop sign indicates the spindle assembly checkpoint that stalls the transition from meta- to anaphase (images of mitotic cells were adapted from (Fernandez et al., 2011)).

Mitosis is by far the shortest phase of the cell cycle and is divided into distinct morphological stages: prophase, prometaphase, metaphase, anaphase and telophase (Figure 1). In prophase, the cell reorganizes its microtubule cytoskeleton. The centrosomes, which build the organizing centers of the microtubule cytoskeleton in interphase and the poles of the mitotic spindle, move apart and the nuclear envelope breaks down (NEBD). During prometaphase the chromosomes condense and are captured by microtubules emanating from the spindle poles. At metaphase, the mitotic spindle aligns the captured chromosomes into a single plane in the middle

1. INTRODUCTION

of the cell, forming the so-called metaphase plate. As soon as all the chromosomes correctly attach and align, the cell transits from metaphase to anaphase, in which the sister chromatids are separated and pulled towards the spindle poles by the microtubules. Telophase marks the end of mitosis, when the chromosomes decondense and the nuclear envelope re-assembles.

Cytokinesis, the separation of the cytoplasm starts with the onset of anaphase. Actin myosin filaments assemble a ring structure at the cell cortex where the metaphase plate was located. The contraction of the actin myosin ring pinches the daughter cells off (Morgan, 2007).

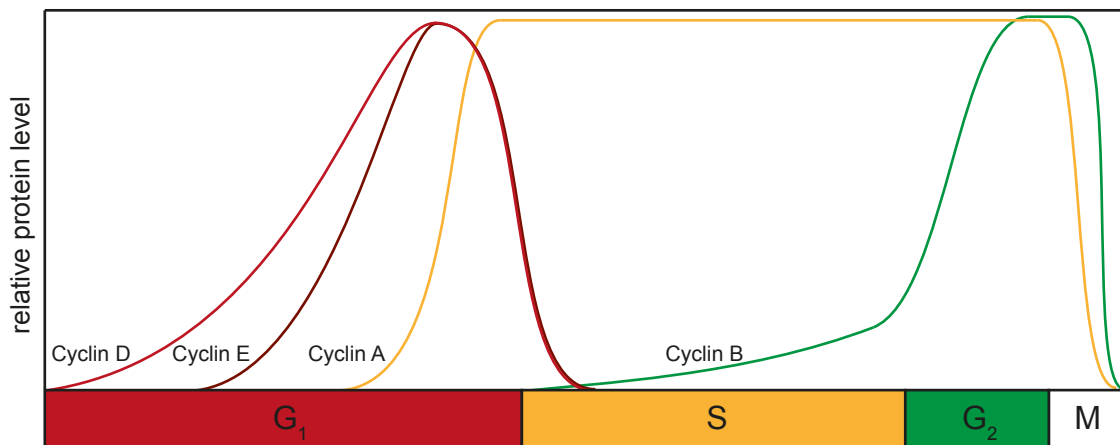


Figure 2: Cyclin levels during the cell cycle

Cyclin D starts to accumulate in early G₁ phase and peaks at the G₁/S transition. The accumulation of Cyclin E follows Cyclin D, also peaking at the G₁/S transition. Cyclin E accumulates with the transition into S phase and drives the DNA replication process. With the onset of mitosis, Cyclin A levels drop. The mitotic Cyclin B slowly accumulates during S phase, then rapidly increases during G₂ before being degraded with the onset of anaphase. Adapted from Truman et al., 2012.

To ensure error-free propagation, cells have developed a finely tuned regulatory network. The core of this network is built by Cyclin-dependent kinases (Cdks) and their activating co-factors, the Cyclin proteins, whose expression is regulated throughout the cell cycle, as their name suggests (Figure 2) (Truman et al., 2001; Morgan, 2007). The modulation of Cyclin protein levels, together with the post-translational regulation of Cdk activity, ensures timely transition throughout the cell cycle (see below). Molecular control mechanisms called checkpoints prevent

1. INTRODUCTION

premature cell cycle progression at G₁/S, G₂/M and meta- to anaphase transition by inhibiting the activity of the corresponding Cdk (Morgan, 2007).

1.1.1 The G₁/S checkpoint

The cellular decision to commit to DNA replication and cell division is determined by the molecular network of the G₁/S checkpoint. To make this decision, external proliferation signals integrate with internal stop-signals. For example, external signals can derive from the JAK-STAT, MAPK/Erk or the Wnt pathway.

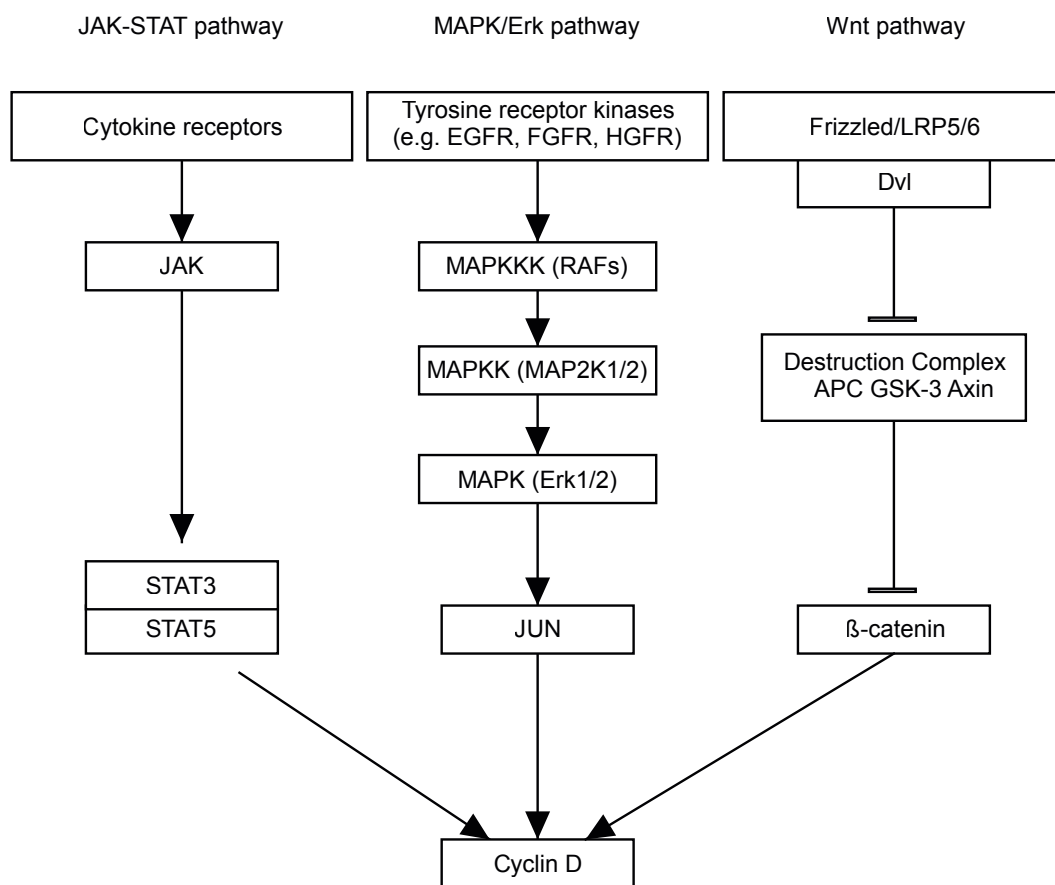


Figure 3: Cyclin D levels are controlled by external signaling pathways

Activated cytokine receptors activate the Cyclin D transcription factors STAT3, or STAT5 via JAK kinases. Growth factors signal through their specific receptor and a kinase-signaling cascade, and drive the transcription of Cyclin D by activating the transcription factor c-Jun. The Wnt-signaling pathway modulates the activity of the destruction complex, which marks its major target β -catenin by GSK-3 phosphorylation for degradation. Free β -catenin activates transcription factors that drive the expression of Cyclin D. Arrows represent activating interactions and T-shaped lines represent inhibitory interactions.

1. INTRODUCTION

Cyclin D is the regulatory subunit of Cdk4 and Cdk6 required to drive the G1/S transition. Cyclin D expression can be triggered via three pathways. Cytokine receptors dimerize upon ligand binding and activate JAK kinases, which subsequently phosphorylate the STAT transcription factors. Phosphorylated STAT proteins form homodimers and trigger the transcription of their target genes; in the case of STAT3 and STAT5, Cyclin D is one of the targets (Rawlings et al., 2004; Klein and Assoian, 2008). Alternatively, growth factors signal through their specific receptor via Ras protein into a mitogen-activated protein (MAP) kinase cascade. The apical Raf or MAP kinase kinase kinase (MAP3K) activates a MAP kinase kinase (MAP2K) activating a MAP kinase (MAPK). MAPK induces Cyclin D expression via transcription factors such as c-Jun (Pearson et al., 2001; Klein and Assoian, 2008). Finally, activation of the Wnt-signaling pathway stops the degradation of β -catenin, thus enabling it to drive the expression of Cyclin D as well as other cell cycle regulators. The Wnt pathway modulates the activity of the destruction complex that marks its major target, β -catenin, for β -TrCP-dependent degradation by GSK-3 phosphorylation. The destruction complex is formed by the APC protein (adenoma polyposis coli) and GSK-3 α or GSK-3 β (Doble et al., 2007). Upon binding of the Wnt protein ligands to Frizzled-receptors, LPR5 or LPR6 is sequestered. LPR5/6, together with the protein Dishevelled, build the platform to inactivate the destruction complex via Axin, freeing β -catenin and thereby promoting Cyclin D expression (Huang and He, 2008) (Figure 3).

Upon Cyclin D accumulation, Cyclin D/Cdk4/6-dependent phosphorylation of RB1 suppresses the inhibitory function of RB1 on the E2F family of transcription factors, which drives the expression of Cyclin E and activates a positive feedback loop where Cyclin E/Cdk2 phosphorylates and thereby inhibits RB1, thus removing the growth

1. INTRODUCTION

factor regulation of S phase transition. However, in the presence of genotoxic stress, p53-induced p21 is able to inhibit this feedback loop. Moreover, stress-activated INK4A family members, including p16, along with p21, are able to directly inhibit Cdk4/6 activity, thus blocking cell cycle progression (Figure 4). Finally, the activation of the E2F family drives cells into the S phase by expressing Cyclin A, which sustains the cell cycle progression by activating Cdk2 and/or Cdk1 (Bartek and Lukas, 2001; Novak et al., 2001).

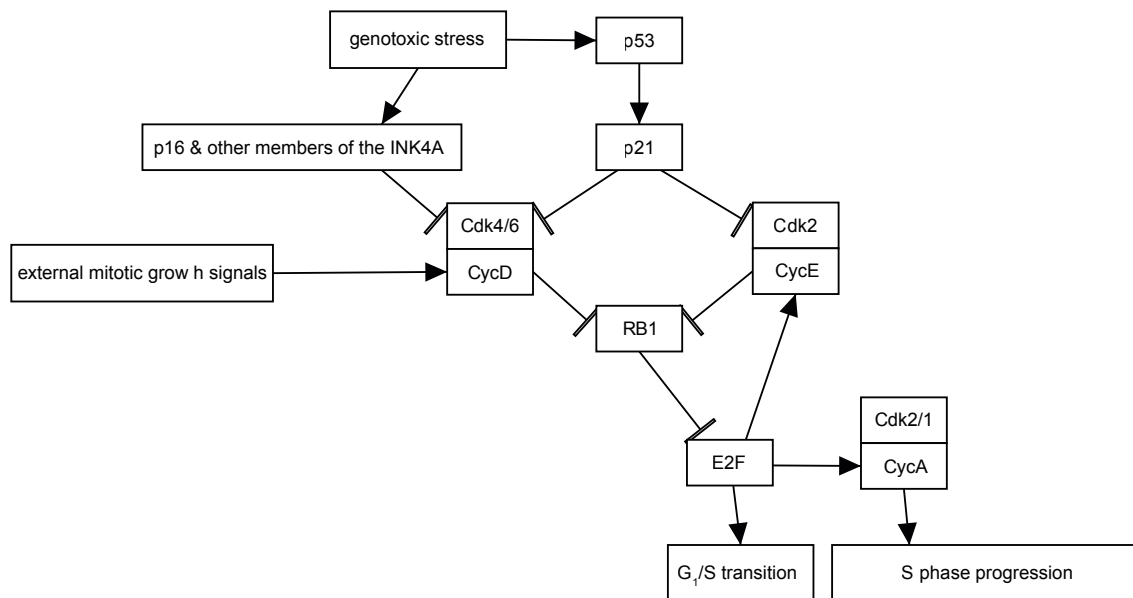


Figure 4: The G₁/S checkpoint

Mitogen stimuli drive the activation of Cyclin D. Cyclin D activates G₁-Cdks 4 and 6, thereby releasing E2F transcription factors by inactivating the Rb protein. A feedback loop with Cyclin E/Cdk2 makes transition into S phase growth factor-independent after reaching a certain threshold of G₁-Cdk activity. The progression to S phase is blocked if genotoxic stress activates p53 or p16 and other members of the INK4A family. p16 and p21, downstream targets of p53, are Cdk inhibitors and thereby stop cell cycle progression. Arrows represent activating interactions and T-shaped lines represent inhibitory interactions.

Taken together, the G₁/S checkpoint is the key rheostat in multicellular organisms regulating cell proliferation in various tissues. Thus, it is logical that several of its components, such as RB, p53 and Cyclin D, are mutated or de-regulated in many tumors contributing to their uncontrolled proliferation, which is a hallmark of cancer (Vermeulen et al., 2003).

1. INTRODUCTION

1.1.2 The DNA-damage checkpoint

DNA double strand breaks (DSB) are recognized by the MRN complex, consisting of Mre11, RAD50 and NBS1, which, in S and G2 phase, initiates the 5'-3' resection that is required for homologous recombination.

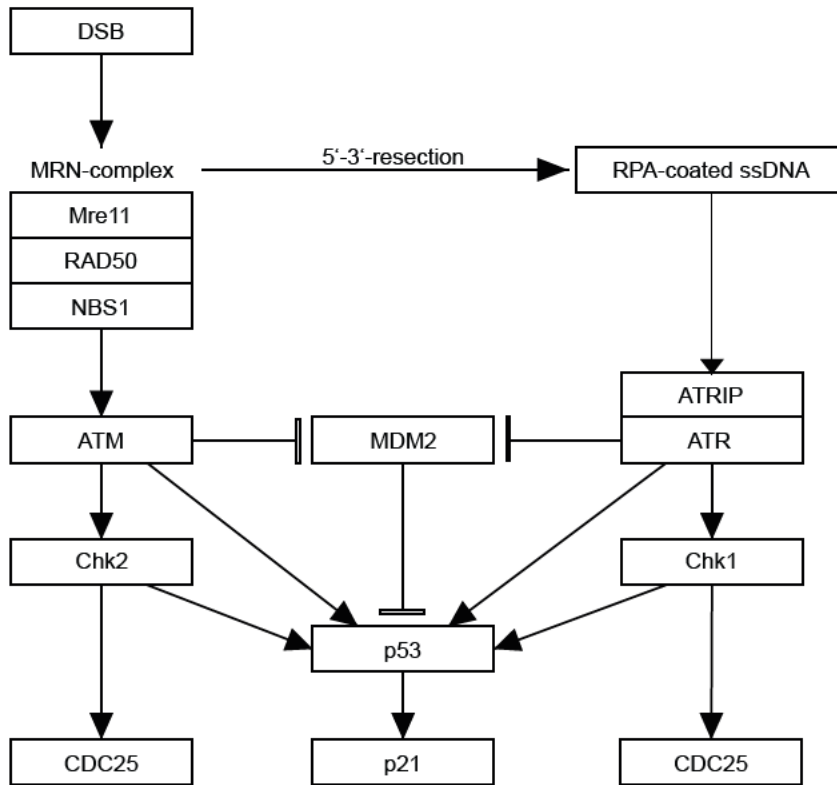


Figure 5: The DNA damage checkpoint

DNA double strand breaks (DSB) or single-stranded DNA (ssDNA) prompt cells to stall their cycle progression until the damage is repaired. The cell cycle arrest-mediating branch of the DNA damage response is shown. The DNA damage signal of the MRN complex is transduced by the apical kinase ATM that phosphorylates the cell cycle effector proteins Chk2, MDM2 and p53. RPA-coated single-stranded DNA generated by the resection of the MRN complex binds and activates the ATRIP/ATR complex. ATR is the apical kinase that transduces the signal to the cell cycle effector proteins MDM2, p53 and Chk1. The inhibition of CDC25 phosphatases by Chk1 and Chk2, and the expression of the Cdk-inhibitor p21, which is a downstream target of p53, mediates cell cycle arrest. Arrows represent activating interactions, T-shaped lines represent inhibitory interactions.

Moreover, the MRN complex recruits the apical kinase ATM to the break site, where it is activated (Kittler et al., 2007; Neumann et al., 2010; Polo and Jackson, 2011; Shiloh and Ziv, 2013). This MRN-dependent activation includes the dissociation of the inactive ATM homodimers and the intermolecular auto-phosphorylation of ATM at serine¹⁹⁸¹ (Bakkenist and Kastan, 2003). Finally, MRN also activates the

1. INTRODUCTION

ATR-mediated response by initiating the 5'-3' resection, which generates single-stranded DNA (ssDNA). RPA coating ssDNA recruits the ATRIP/ATR complex (Symington and Gautier, 2011). ATM and ATR phosphorylate the histone H2AX on serine¹³⁹. This phosphorylation is the most commonly recognized marker for DSBs (γ -H2AX) and its dephosphorylation is involved in the termination of cell cycle arrest (Chowdhury et al., 2005 & 2008; Nakada et al., 2008). Chk1, which is activated by an ATR-, and Chk2, activated by an ATM-dependent phosphorylation, stabilize p53 by phosphorylating the serine²⁰ residue. ATM and ATR also phosphorylate p53 at serine²⁰, which, together with phosphorylation of the E3-ligase MDM2 that targets p53 for 26S-proteasomal degradation, inhibit the p53-MDM2 interaction, thus blocking p53 degradation. Moreover, ATM and ATR phosphorylate serine¹⁵ of p53, stimulating the transactivation of p53 as well as weakening the MDM2-p53 interaction (Abraham, 2001). The Cdk-inhibitor p21, an important downstream target of p53, and the inhibition of the cell cycle promoting phosphatases CDC25 by Chk1 and Chk2, execute the cell cycle arrest by keeping the corresponding Cyclin-Cdk complex inactive.

1.1.3 The G₂/M checkpoint

Cells are driven from G₂ into mitosis by a switch-like increase of Cdk1 activity. To prevent cells entering mitosis with damaged or un-replicated DNA, the G₂/M checkpoint keeps the Cdk1 activity low as long as DNA damage is not repaired and the checkpoint is activated.

1. INTRODUCTION

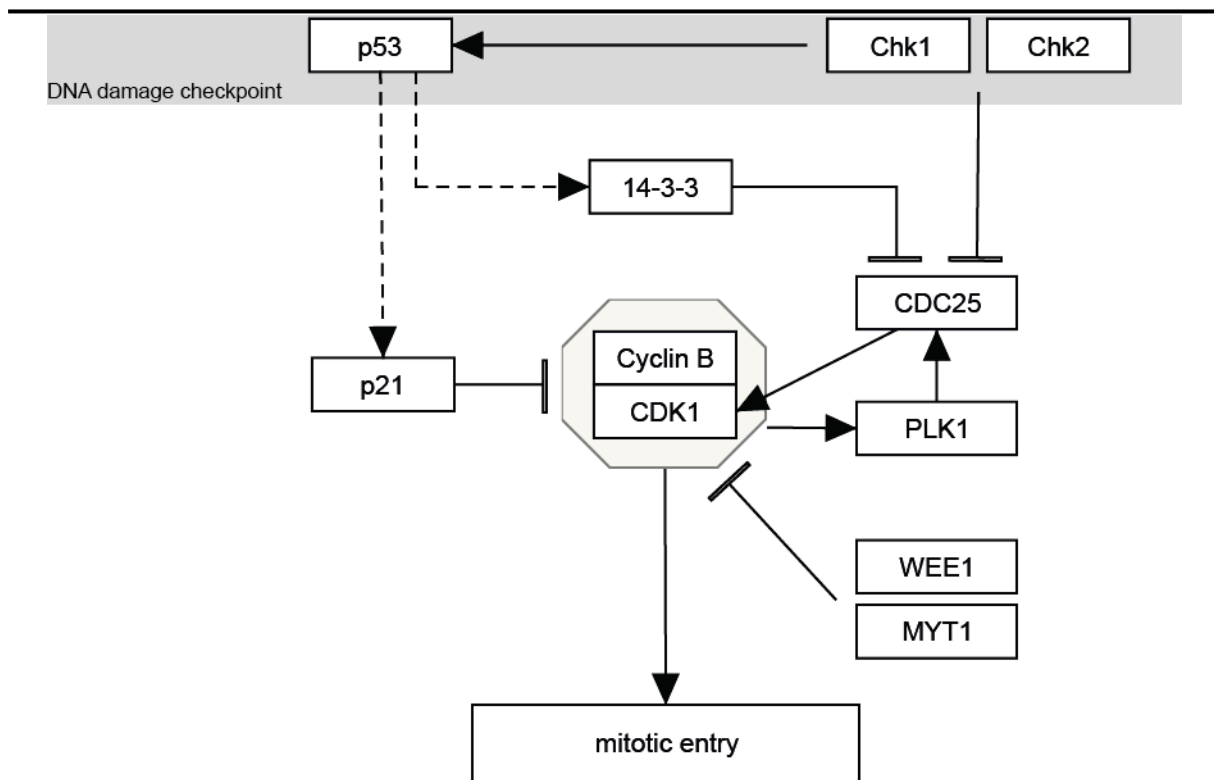


Figure 6: The G₂/M checkpoint

The regulatory network of the G₂/M checkpoint, which controls the activity of Cdk1/Cyclin B, is visualized. The gray background highlights the effector proteins, p53, Chk1 and Chk2 of the DNA damage checkpoint. Dashed lines represent transcriptional activation, arrows a direct activating interaction and T-shape line a direct inhibitory interaction.

To gain the full Cdk1/Cyclin B activity necessary to enter mitosis, cells have to execute two regulatory processes: CDC25 phosphatases have to remove the Wee1- and Myt1-mediated inhibitory phosphorylation on Cdk1, and the inhibition of the Cdk1/Cyclin B complex by p21 has to be abrogated (Figure 6). This is only achieved, after the p53-mediated expression of p21 and 14-3-3 σ ceases and Chk1 and Chk2 are no longer active. Further, 14-3-3 σ inhibits CDC25 phosphatases phosphorylated by Chk1 and Chk2 via cytoplasmic retention. Finally, Chk1 and Chk2 prime CDC25 phosphatases for ubiquitin-mediated degradation. Once the trigger from the DNA damage checkpoint has passed, Cdk1/Cyclin B-mediated Plk1 activates CDC25 phosphatases. This positive feedback loop leads to a switch-activation of Cdk1 and entry into mitosis (Stark and Taylor, 2006).

1. INTRODUCTION

1.1.4 The spindle assembly checkpoint

To safeguard the daughter cell from becoming aneuploid, the mitotic or spindle assembly checkpoint (SAC) stalls the mitotic progression into anaphase until each chromosome is attached to microtubule bundles emanating from the opposing spindle poles. Therefore, microtubules are anchored to the chromosomes by huge protein structures called kinetochores, which generate the SAC stop-signal unless they are properly attached to the microtubules and tension is formed between sister kinetochores by the forces pulling from opposite poles (Musacchio and Salmon, 2007).

The exact mechanism by which the SAC is established is still a matter of investigation, but in summary, un-attached kinetochores require MPS1 to recruit the RZZ complex (Rod, Zw10, Zwilch), which together with MPS1 and the Bub proteins (Bub1, BubR1, Bub3) recruit the Mad1-Mad2 complex (Lara-Gonzalez et al., 2012). Mad2 exists in two conformations: an open inactive one and a closed active one; Mad2 bound to Mad1 is in its closed active conformation and is capable of activating other Mad2 molecules that are in the inactive open conformation and not bound to Mad1, by converting these to the active closed conformation (Vink et al., 2006). Free Mad2 in its closed active conformation binds Cdc20, an activating subunit of the anaphase-promoting complex (also called cyclosome, APC/C). Mad2, together with Cdc20, BubR1 and Bub3, forms the mitotic checkpoint complex (MCC), which binds and inhibits the APC/C (Nezi and Musacchio, 2009; Lara-Gonzalez et al., 2012) (Figure 7, top panel).

The microtubule-kinetochore interaction is stabilized when the microtubules emanating from opposing spindle poles attach to the sister kinetochore in a manner that generates both inter- and intra-kinetochore tension. Microtubule-kinetochore interactions that are incapable of generating tension are dissolved in an

1. INTRODUCTION

Aurora B-dependent manner; and thus, generate un-attached, MCC-producing kinetochores (Rago and Cheeseman, 2013) (Figure 7, middle panel).

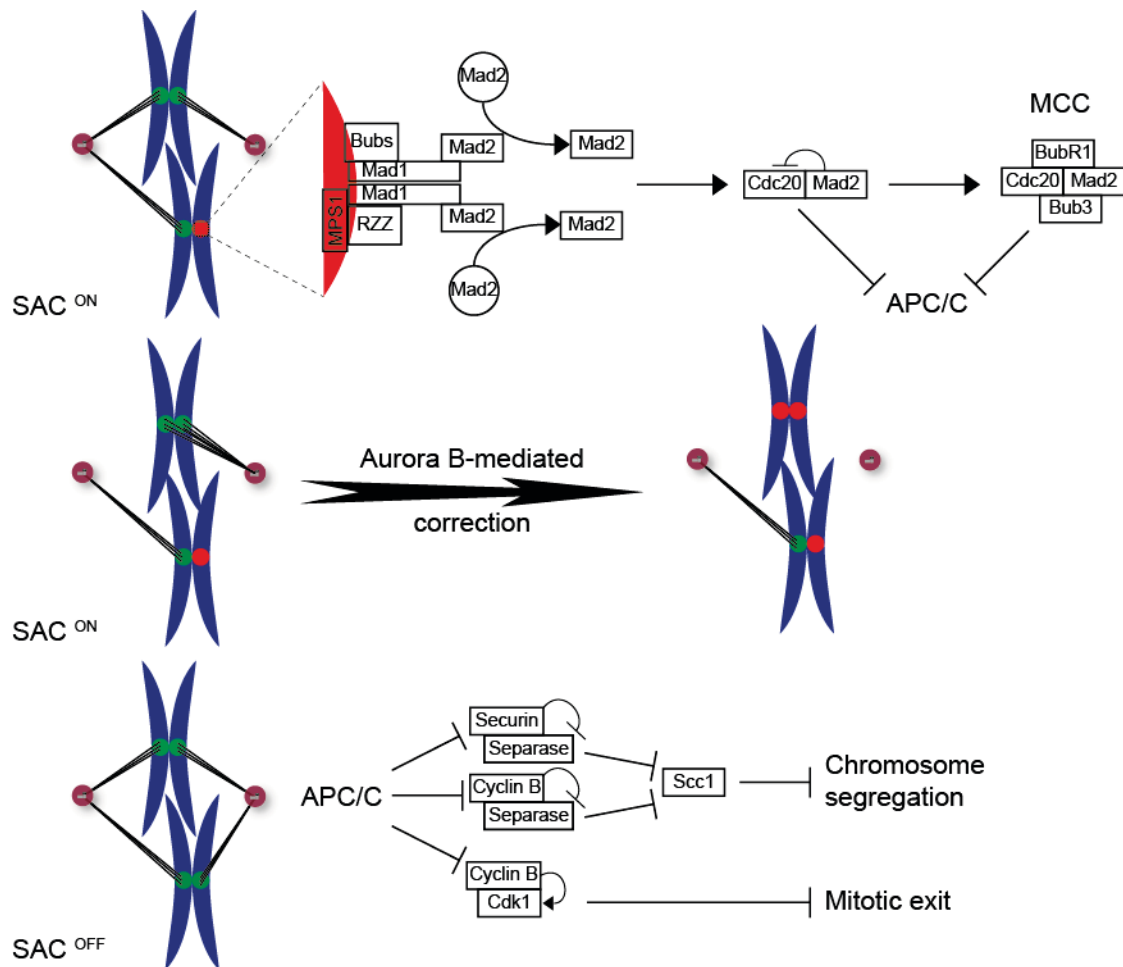


Figure 7: The spindle assembly checkpoint

The fundamental concepts of the SAC are visualized. The top panel shows that un-attached kinetochores recruit Mad1 and Mad2 in MPS1-dependent manner, the RZZ complex and the Bub proteins. The Mad1-Mad2 complex converts the inactive *open*-Mad2 into the active *closed*-Mad2 to inhibit the APC/C by forming the mitotic checkpoint complex MCC and sequestering Cdc20, the activating subunit of the APC/C. The panel in the middle shows the SAC activation by faulty tensionless kinetochore-microtubule connections, which are resolved by Aurora B and therefore creating un-attached kinetochores. The bottom panel visualizes how the APC/C activates Separase and inactivates Cdk1 by degrading Cyclin B and Securin, which leads to chromosome segregation and mitotic exit. The sister chromatids depicted in blue with green or red circles represent attached and un-attached kinetochores, respectively. Black lines emanating from the spindle poles in dark red represent microtubules. Arrows represent activations and T-shape lines inhibition.

Once all kinetochores are stably attached to microtubules emanating from opposing spindle poles, the SAC is switched off and the Mad1-Mad2 complex is stripped from the kinetochore via the dynein-mediated removal of the RZZ complex. The Cdc20-activated APC/C drives the transition into anaphase by targeting Securin and

1. INTRODUCTION

Cyclin B for proteasomal degradation. The degradation of these two proteins is a key event for progression into anaphase for two reasons: first, both proteins inhibit Separase whose activity is required to open the Cohesin ring, which holds sister chromatids together and prevents premature chromosome segregation. Therefore, Separase cleaves the Kleisin subunit Scc1 and triggers chromosome segregation. Secondly, Cdk1 activity drops with the degradation of Cyclin B and releases the daughter cells from mitosis into G₁ (Figure 7, bottom panel).

The SAC ensures that the chromosomes carrying genetic information are equally distributed into the daughter cells during mitosis (Foley and Kapoor, 2013). Mouse models demonstrate that increased CIN and tumorigenesis are the consequences of a compromised SAC (Schvartzman et al., 2011). Further, it has been shown that mosaic variegated aneuploidy (MVA), a disorder with a high risk of childhood cancer, is caused by a gene mutation that renders the SAC component BubR1 inactive (Micale et al., 2007). This convincingly shows that the SAC plays an important role in preventing CIN and tumorigenesis despite the fact that only a low number of human tumors with a compromised SAC have been found so far.

Taken all together, the mechanisms that control the cell cycle and in particular the ones that are important for the faithful chromosome segregation and cell division are in the focus of many studies that investigate tetraploidy in context of tumorigenesis including the ones presented in this work.

1. INTRODUCTION

1.2 The links between tumorigenesis and tetraploidization

Aneuploidy is a hallmark of solid tumors; the chromosome numbers of most human tumors range between diploidy and tetraploidy. Tumors frequently contain hypertriploid or hypotetraploid chromosome sets (Figure 8). This observation fits the hypothesis that tetraploidization is a key step during tumorigenesis (Shackney et al., 1989; Storchova and Pellman, 2004).

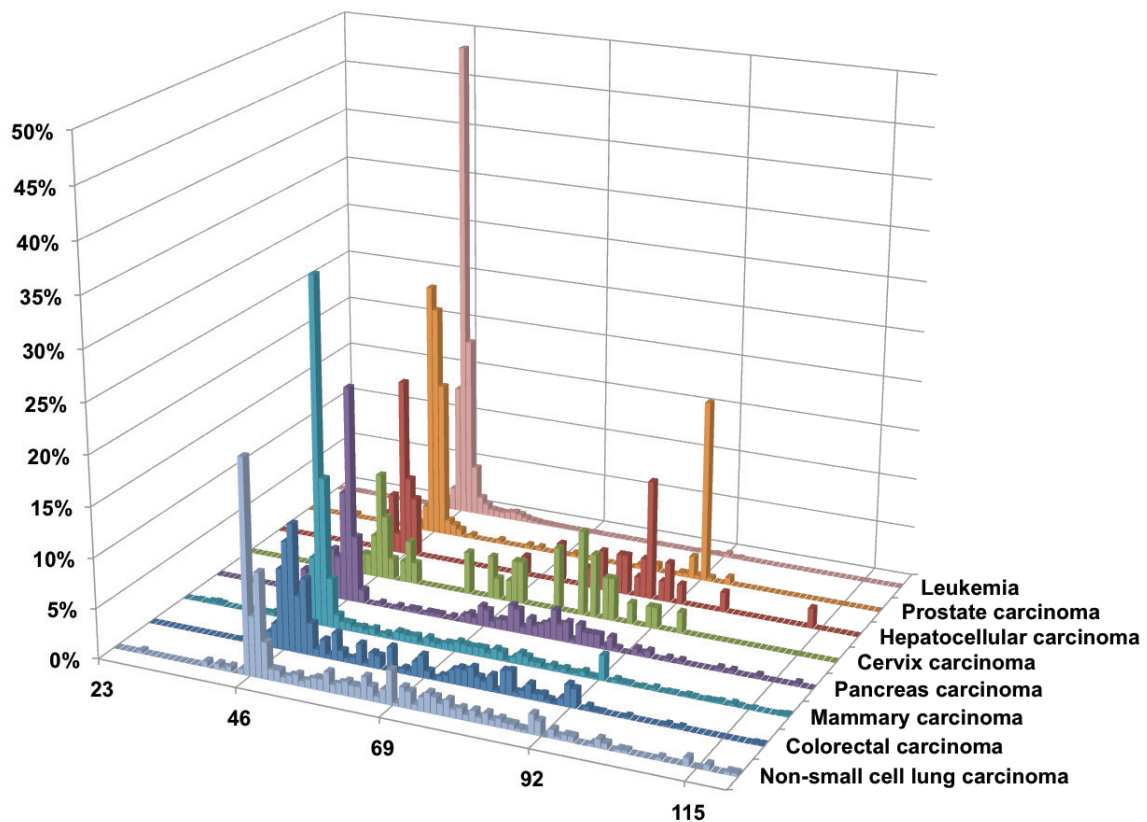


Figure 8: Distribution of chromosome number in common cancers

The percentage of tumors plotted against the corresponding maximum chromosome number reveals that diploid or near-diploid karyotypes dominate across cancer types. A high percentage of tumors with near-triploid or near-tetraploid chromosome numbers suggests that changes in whole chromosome sets are frequent in cancers. The Mitelman Database of Chromosome Aberrations in Cancers was used as a source of the data (<http://cgap.nci.nih.gov/Chromosomes/Mitelman>). Adopted from (Storchova and Kuffer, 2008).

This chapter summarizes first the mechanisms leading to tetraploidization, second the evidence that tetraploidization drives tumorigenesis, and finally the known cellular mechanisms that restrict the proliferation after tetraploidization.

1.2.1 Aberrant tetraploidization

Aberrant tetraploidization of somatic cells can occur by either one of three main mechanisms: cell-cell fusion, mitotic slippage or failure to complete cytokinesis (Figure 9).

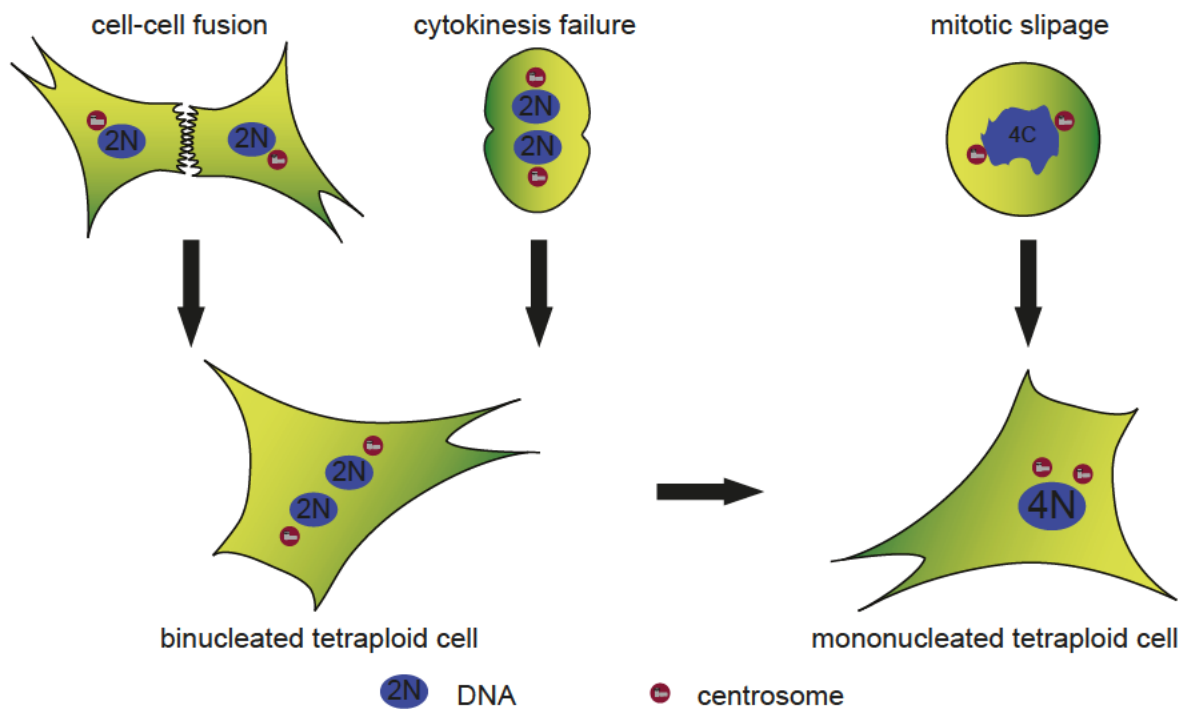


Figure 9: Tetraploidization mechanisms

Cell-cell fusion and failure of cytokinesis generate binucleated cells that contain two centrosomes. Binucleated cells can form mononucleated tetraploids after successful passage through the next mitosis. Mitotic slippage is a cellular adaptation to persistent mitotic arrest. Cells bypass anaphase, telophase and cytokinesis, and progress into the next G1 phase without correcting the mitotic error that triggered the arrest. Cells that are derived from mitotic slippage contain either a single or fragmented tetraploid nucleus that is accompanied by two centrosomes. 2N, diploid nucleus; 4N, tetraploid nucleus; 4C, diploid nucleus with replicated chromosomes. Adopted from (Storchova and Kuffer, 2008)

Cell-cell fusion can be induced by enveloped viruses, which comprise common human pathogenic viruses as well as oncogenic viruses. Enveloped viruses employ proteins that have the ability to fuse biological membranes to enter host cells. Therefore, enveloped viruses can induce fusion of cells leading to the formation of binucleated heterokaryons with two centrosomes, as seen in both *in vitro* and *in vivo* models (Dimitrov, 2004; Marsh and Helenius, 2006; Duelli and Lazebnik, 2007).

1. INTRODUCTION

Tetraploidization may also occur due to aberrant cell division. Bulk chromatin, or even a single lagging chromosome trapped in the cleavage furrow can prevent cells from completing cytokinesis (Mullins and Biesele, 1977; Shi and King, 2005). Abnormal spindle positioning and movements may also interfere with cytokinesis; it was shown that defects in spindle anchoring or spindle assembly lead to tetraploidization (Reverte et al., 2006; Caldwell et al., 2007). The result of cytokinesis failure is a single binucleated cell with two centrosomes.

Cells that are not able to resolve a mitotic defect that persistently activates the SAC will exit from mitosis without undergoing anaphase and cytokinesis; this phenomenon is called “mitotic slippage” (Brito and Rieder, 2006). Mitotic slippage produces tetraploid cells with a single nucleus accompanied by two centrosomes (Elhajouji et al., 1998; Lanni and Jacks, 1998).

Tetraploid cells can be found with variable frequencies (0.5 % to 20 %) in nearly every human tissue (Biesterfeld et al., 1994) and list of routes leading to tetraploidization is growing, thus raising the possibility that unscheduled tetraploidization occurs frequently in normal tissues. Therefore, it has been suggested spontaneous unscheduled tetraploidization might be far more frequent than an oncogenic gene mutation (Storchova and Kuffer, 2008).

1.2.2 Tetraploidy-driven tumorigenesis

By now a solid body of evidence suggests that tetraploidization can drive tumorigenesis. First, it was shown that mice overexpressing the mitotic kinesin KIF11 (also known as Eg5) or the SAC component MAD2 accumulated tetraploid cells and developed tumors in various tissues (Castillo et al., 2007; Sotillo et al., 2007). In case of MAD2, even transient overexpression was sufficient to trigger tumorigenesis (Sotillo et al., 2007). Moreover, *in vitro* and mouse experiments showed that the

1. INTRODUCTION

overexpression of the mitotic kinase Aurora A results in cytokinesis failure as well as in a shortened tumor-free survival of the mice (Meraldi et al., 2002; Wang et al., 2006). In human cancers, Aurora A is frequently overexpressed and correlates with more aggressive tumor progression and increased CIN (Katayama et al., 2003).

Second, the analysis of known tumor suppressor genes revealed that mutations leading to a loss of function may trigger tetraploidization. For example, it has been shown that defect in the DNA repair gene BRCA2 prompts cleavage failure at the end of mitosis in human cancer cells as well as mouse fibroblasts. Thus, BRCA2 deficiency leads to the accumulation of binucleated tetraploid cells and polyploid cells *in vivo* and *in vitro* (Daniels et al., 2004).

Similar observations have been made for the well-established tumor suppressor gene APC, whose loss of function due to truncating mutations is an early event during tumorigenesis of colorectal cancers. Patients with a germline mutation in the APC gene suffer from familial adenomatous polyposis (FAP; earlier known as Gardner syndrome) and develop thousands of polyps in their intestine, quickly followed by the development of colorectal cancer (Kinzler and Vogelstein, 1996; Polakis, 1997). Although the carcinogenic potential of APC mutations is usually attributed to APC's role in β -catenin-dependent Wnt signaling (Clevers, 2006), it was convincingly demonstrated that APC mutations also affect the anchoring of mitotic spindles. Affected cells subsequently fail to establish a proper cleavage plane due to the rotation of the mitotic spindle, causing cytokinesis failures and thereby tetraploidization (Caldwell et al., 2007; Dikovskaya et al., 2007). This finding is in concordance with the observed spontaneous tetraploidization of primary fibroblasts from patients diagnosed with Gardner syndrome (FAP) (Danes, 1976).

Third, tetraploid cells are frequently found in tumors of all stages (Figure 8) and in pre-malignant conditions. Before gross aneuploidy, tetraploid cells are detected

1. INTRODUCTION

within neoplastic lesions of Barrett's esophagus that precede esophageal adenocarcinoma (Galipeau et al., 1996; Barrett et al., 2003; Maley, 2007). Similarly, the tetraploid cells were also detected in early stages of cervical tumorigenesis (Olaharski et al., 2006). Recently, the gene copy number analysis of 4934 primary cancer specimens across 11 cancer types revealed that 37% underwent tetraploidization at some point during tumorigenesis (Zack et al., 2013).

Fourth, every virus with known human oncogenic potential (Human papilloma virus, Epstein–Barr virus, HTLV-1, hepatitis B and C virus) induce tetraploidization by cell-cell fusion (Duelli and Lazebnik, 2007; Hu et al., 2009). Indeed, transgenic mice that express T-antigen of the SV40 (simian virus 40) in pancreas first accumulate tetraploid cells before aneuploid tumors form (Ornitz et al., 1987). Another study used the Mason-Pfizer Monkey Virus (MPMV), which is also found in humans, but without cytostatic or cytotoxic effect. Tetraploid cells generated by the MPMV-triggered fusion of cells expressing the oncogene HRAS with cells expressing E1A displayed CIN and were tumorigenic in xenograft mouse models. On the other hand, did the combined expression of the oncogenes HRAS and E1A in diploid MPMV-infected cells not trigger any CIN nor tumor formation (Duelli et al., 2005 & 2007).

Finally, the most direct experimental evidence that tetraploidization initiates tumorigenesis has been provided by a study that monitored tumor formation in nude mice comparing subcutaneous injection of *p53*-null mammary epithelial-gland cells that were either tetraploid or diploid. Ten out of 39 animals developed tumors at the sites where tetraploid cells had been injected, but none of the animals developed tumors at the injection site of isogenic diploid cells that underwent identical procedure as the tetraploid cells. The cells isolated from the tumors displayed near-tetraploid karyotypes with significant whole-chromosomal aneuploidy and several chromosomal rearrangements (Fujiwara et al., 2005). Similarly, intraperitoneal injections of

1. INTRODUCTION

tetraploid mouse ovarian surface epithelia cells (MOSECs) that were generated by long-term *in vitro* passaging caused the development tumors, but the injection of short-term *in vitro* passaged diploid MOSECs did not (Lv et al., 2012).

Taken all together, the data provides compelling evidence that tetraploidization plays a key role in development of solid tumors. However, the findings also underscore that tetraploidy-driven tumorigenesis requires the malfunction of a gatekeeper gene, like TP53 or APC. This suggests that metazoan cells have developed protection mechanisms against the proliferation of cells that underwent unscheduled tetraploidization.

1.2.1 Mechanisms preventing cell proliferation after tetraploidization

To date, only a few studies have directly addressed, which genes prevent the proliferation of mammalian cells after tetraploidization. Thus far, only TP53 (p53) has been repeatedly confirmed to be required to suppress cell proliferation after tetraploidization; additionally, CDKN1A (p21), CDKN2A (p16) and RB1 (Rb) have also been implicated (Cross et al., 1995; Andreassen et al., 2001; Meraldi et al., 2002; Fujiwara et al., 2005). Despite the confirmed role of p53 in suppressing cell proliferation after tetraploidization, it has been shown that binucleated tetraploid cells with functional p53 pathway are capable of completing at least one tetraploid cell cycle as well (Uetake and Sluder, 2004). This raised the question when and how human cells arrest after tetraploidization.

One possible trigger might be the time cells spend in mitosis; untransformed human retinal pigment epithelial (hTERT RPE-1) enter a p53-dependent post-mitotic G₁ arrest mediated by the p38/MAPK stress kinase, if they were mitotically blocked by the microtubule inhibitor Nocodazole in mitosis for more than 1.5 h (Uetake and

1. INTRODUCTION

Sluder, 2010). Thus, cells might enter a post-mitotic G1 arrest due to the time they spend in mitosis after tetraploidization, because mitosis in tetraploid hTERT RPE-1 takes around 50 min after tetraploidization, in contrast to 20 min of diploid mitosis (Yang et al., 2008).

Another possibility is that cells acquire DNA damage during or after tetraploidization that prevents further cell proliferation. For example, the prolonged tetraploid mitosis could eventually lead to such DNA damage. Human diploid cells that spend 6 h or more in mitosis accumulated significant amounts of DNA damage (Dalton et al., 2007; Quignon et al., 2007). Another possibility is that after tetraploidization, an increased number of lagging chromosomes are damaged in the cleavage furrow due to the elevated missegregation after multipolar mitosis caused by the extra centrosomes that cells contain after tetraploidization (Ganem et al., 2009; Janssen et al., 2011).

A faulty mitosis might also directly signal a cell cycle arrest. Thus, it was shown in mouse embryonic fibroblasts that the incidence of survival after chromosome missegregation correlates with the expression levels of Bub1. Compared to wild-type MEFs, MEFs with reduced Bub1 escape p53-mediated cell death more frequently (Jeganathan et al., 2007). In humans, the related BubR1 proteins was found to be downregulated in colorectal tumors and the ectopic expression of a dominant-negative BubR1 mutant in cells that underwent tetraploidization lead to tumor growth in xenograft models (Shin et al., 2003). Furthermore, it has been reported that BubR1 induced the phosphorylation and stabilization of p53 (Ha et al., 2007).

On the other hand, a faulty mitosis could trigger cell cycle arrest indirectly. It was reported that the missegregation of a single chromosome in human diploid cells lead

1. INTRODUCTION

to the accumulation of p53 and its target, the cell cycle inhibitor p21. The inhibition of p53 as well as p38 function was necessary for the accumulation of aneuploid cells after induced chromosome missegration. The trigger for p38-activated p53-stress response is still unclear; however it was hypothesized that a proteotoxic stress caused by the imbalanced gene copy number might activate the p38 stress kinase (Thompson and Compton, 2010).

Together, the data obtained from these studies suggest that passage throught the tetraploid mitosis is critical for the decision about the fate of cells after tetraploidization.

2. RESULTS

2.1.1 Abnormal mitosis triggers p53-dependent cell cycle arrest in human tetraploid cells

Kuffer, C., Kuznetsova, A.Y., and Storchova, Z. (2013). Abnormal mitosis triggers p53-dependent cell cycle arrest in human tetraploid cells. *Chromosoma*.

This publication addresses the previously unanswered questions of when and why cells arrest in a p53-dependent manner after tetraploidization.

By long-term live cell imaging of individual cells after tetraploidization, it was shown that HCT116 cells completed one cell cycle, but arrested and died in a p53-dependent manner after exiting the first tetraploid mitosis. The main trigger for this arrest came from a defective mitosis caused by spindle multipolarity and massive chromosome missegregation. In contrast, no correlation was observed between length of mitosis and the arrest after tetraploidization, nor did the presence of DNA double strand breaks correlate with the activation of p53. However, the amount of oxidative DNA damage increased co-linearly with p53 within 24 h after tetraploidization. Moreover, the amount of oxidative DNA damage and p53 also correlated at an individual cell level.

ATM has previously been shown to activate p53 in situations with elevated ROS level and increased oxidative DNA damage due to chromosome missegregation perturbing the SAC (Li et al., 2010). Congruently, the inhibition of ATM reduced the activation of p53 and increased the proliferation of cells after tetraploidization.

2.2 Myocardin related transcription factors are required for coordinated cell cycle progression

Shaposhnikov, D., Kuffer, C., Storchova, Z., and Posern, G. (2013). Myocardin related transcription factors are required for coordinated cell cycle progression. *Cell Cycle* 12, 1762–1772.

This publication addresses the question, which effect MRTFs have on cell cycle regulation and ploidy. It shows that clonal populations raised from NIH3T3 cells stably depleted of Myocardin-related transcription factors A and B (MRTFs) were frequently tetraploid or aneuploid, despite the fact that transient depletion of MRTFs did not increase the number of binucleated cells. However, lead the depletion of MRTFs in NIH3T3 cells to an increase of cells with nuclear buds or micronuclei. Depletion of MRTFs increased the expression of Cyclin D1, which is linked to the cell cycle progression from G₁ into S phase. Moreover, in the absence of growth factors, MRTFs-depleted cells entered S and G₂ phase more frequently than control-depleted cells. Accordingly, the expression of the cell cycle inhibitors p27Kip1, p18Ink4c and p19Ink4d were decreased in MRTFs-depleted cells. However, this did not lead to an increased proliferation of MRTFs-depleted cells, and correlates with the observation that the expression of the cell cycle inhibitor p21 was also increased in these cells. Under normal growth conditions, the MRTFs-depleted cells showed an impaired proliferation accompanied with a significantly shortened G₁ phase and a slightly extended S/G₂ phase.

These results suggest an important and complex role for MRTFs in maintaining proper cell cycle progression and genomic stability.

2.3 A genome-wide screen identifies genes enhancing, as well as restricting, cellular proliferation after tetraploidization.

2.3.1 Experimental Setup

About 80 % of the HCT116 cells that underwent a *Di-hydro-Cytochalasin D* (DCD) induced cytokinesis failure followed by tetraploidization progress through first tetraploid cell cycle and enter the first tetraploid mitosis about 10 h after the DCD removal. Approximately 50 % of these tetraploid HCT116 cells arrest after the first tetraploid mitosis due to chromosome segregation errors (Kuffer et al., 2013). Most of the cells that do not arrest enter the next mitosis between 24 h and 47 h after the DCD washout (Figure 10). This suggests that the largest difference and therefore the largest dynamic range between proliferating and arresting cells occurs 24 h after the DCD removal, because at that time most of the proliferating tetraploid cells are in G₂/M phase, from which they can be distinguished from the cells arresting after the first mitosis in G₀/G₁ phase. Thus, the timing of the 1st and 2nd mitosis after tetraploidization allows us to determine whether gene functions affect the cell proliferation after tetraploidization by RNA interference screen. Therefore, we chose to transfect the HCT116 cells within the time frame 38 h – 62 h before the DCD washout, which is 20 h – 44 h before the DCD treatment.

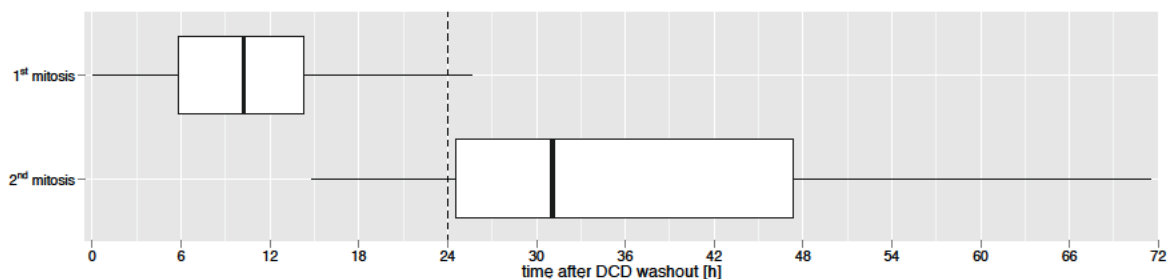


Figure 10: Time of mitotic entry of tetraploid cells after DCD washout

Boxplot of the time tetraploid cells enter mitosis after DCD washout. The vertical dashed line represents the time point of the readout of the tetraploid arrest.

2. RESULTS

The precondition that the cells must be transfected prior the DCD treatment makes purification of tetraploid cells by flow cytometry for genome-wide approach impossible. Even though cell cycle profiling should in principal be suitable to detect differences in proliferation of tetraploid cells (Kittler et al., 2007; Theis et al., 2009); in this case however, where tetraploid cells are mixed with diploid cells the cell cycle profiling based solely on DNA content analysis was not robust enough for a high-throughput analysis (data not shown).

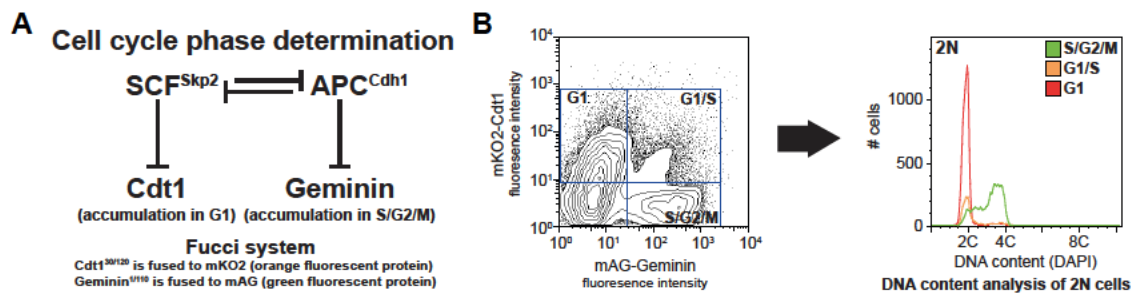


Figure 11: HCT116 Fucci

A: Schematic depiction of the Fucci cell cycle sensors. B: Flow cytometry characterization of the HCT116 Fucci cell line. Left panel shows the cell cycle staging by a 2D density plot of the fluorescence intensities of the Fucci cell cycle probes. Right panel show the cell cycle histograms of the determined cell cycle stages.

To increase the robustness of the assay, the DAPI-based DNA content analysis was supported with genetically encoded cell cycle sensors called Fucci. The Fucci G₁ sensor consists of the N-terminus of Cdt1 fused to mKO2 (an orange fluorescent protein) and is therefore degraded in S, G₂ and M phase by the SCF complex. The Fucci G₂ sensor consists of the N-terminus of Geminin fused to mAG and is therefore degraded between anaphase and S phase by the APC/C complex (Figure 11A) (Sakaue-Sawano et al., 2008). We generated the HCT116 Fucci cell line that expresses both these cell cycle sensors. The flow cytometry analysis of HCT116 Fucci cells shows four distinct populations: a G₁ positive for Fucci G₁, a G₁/S positive for Fucci G₁ and G₂, a S/G₂/M positive for Fucci G₂ and a population expressing neither Fucci G₁ nor G₂ (Figure 11B).

2. RESULTS

2.3.2 Primary screen

The primary screen for novel factors that affect the proliferation of tetraploid cells was carried out in 5 batches. In each batch, HCT116 Fucci cells were seeded into black 384-well glass plates on top of the esiRNAi transfection mix and treated 24 h later with the 0.75 μM DCD for 18 h. After the DCD removal, the cells were cultured for additional 24 h and subsequently fixed and imaged. After segmenting the nuclei in each image, the nuclei were assigned to one of six distinguished cell cycle classes 2CG1, 2CS, 4CG2, 4CG1, 4CS and 8CG2 according to what DNA content they harbored and which Fucci cell cycle probe they expressed (Figure 12).

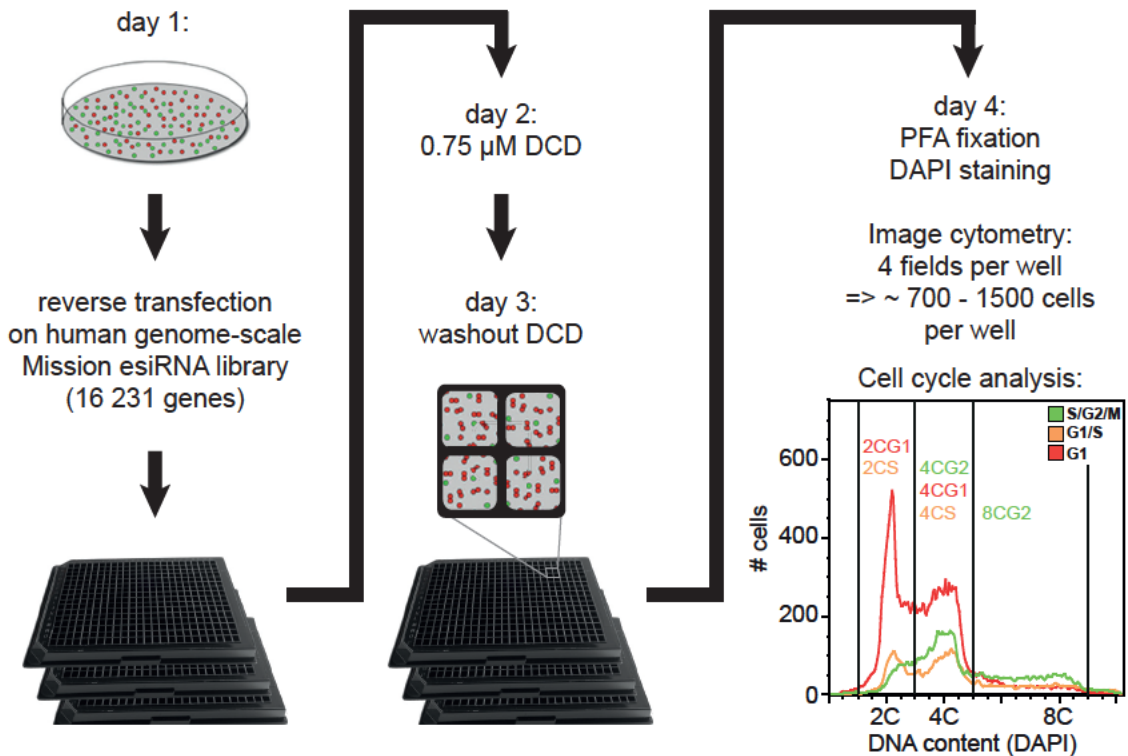


Figure 12: Scheme of experimental workflow

At day 1 the HCT116 Fucci cells were reverse-transfected in 384-well black glass bottom plates. The next day *Di-hydro-Cytochalasin D* (DCD) diluted in growth medium was added to a final concentration of 0.75 μM . 18 h later the DCD was washed out and the mixture of binucleated tetraploid cells and mononucleated diploid cells was further incubated for one day. After fixing with paraformaldehyde and staining with DAPI, 4 fields per well were acquired. After segmenting the images to determine the nuclei, the fluorescence intensity of the DAPI and the Fucci signals of each nucleus were quantified. The cell cycle profiles of cells expressing the FucciG₁, FucciG₂ or both Fucci cell cycle probes were divided into cells with 2C, 4C or 8C DNA content.

2. RESULTS

Cells that did not express any Fucci cell cycle sensor were excluded from the analysis. For each of the six classes, the relative abundance was calculated and transformed into a Z^* -score value. The Z^* -score transformation was performed for each cell cycle class by dividing the difference between its relative abundance in a particular well of a plate and the median of the whole plate by the median absolute deviation (MAD) (Zhang, 2011). Control wells transfected with esiRNA targeting either TP53 or KIFC1 were excluded from the calculation of the median and MAD of the plate.

The plate average or plate median can be used instead of classic non-targeting negative controls based on the assumption that the vast majority of the tested genes in a genome-wide library are not involved in the studied process (Theis and Buchholz, 2011). The Z^* -score calculation normalizes the individual assay plates against each other (Figure 13) as well as the medians and variance of the different cell cycle classes against each other; thus all cell cycle classes have an isotropic variance after the calculation (Figure 14).

2. RESULTS

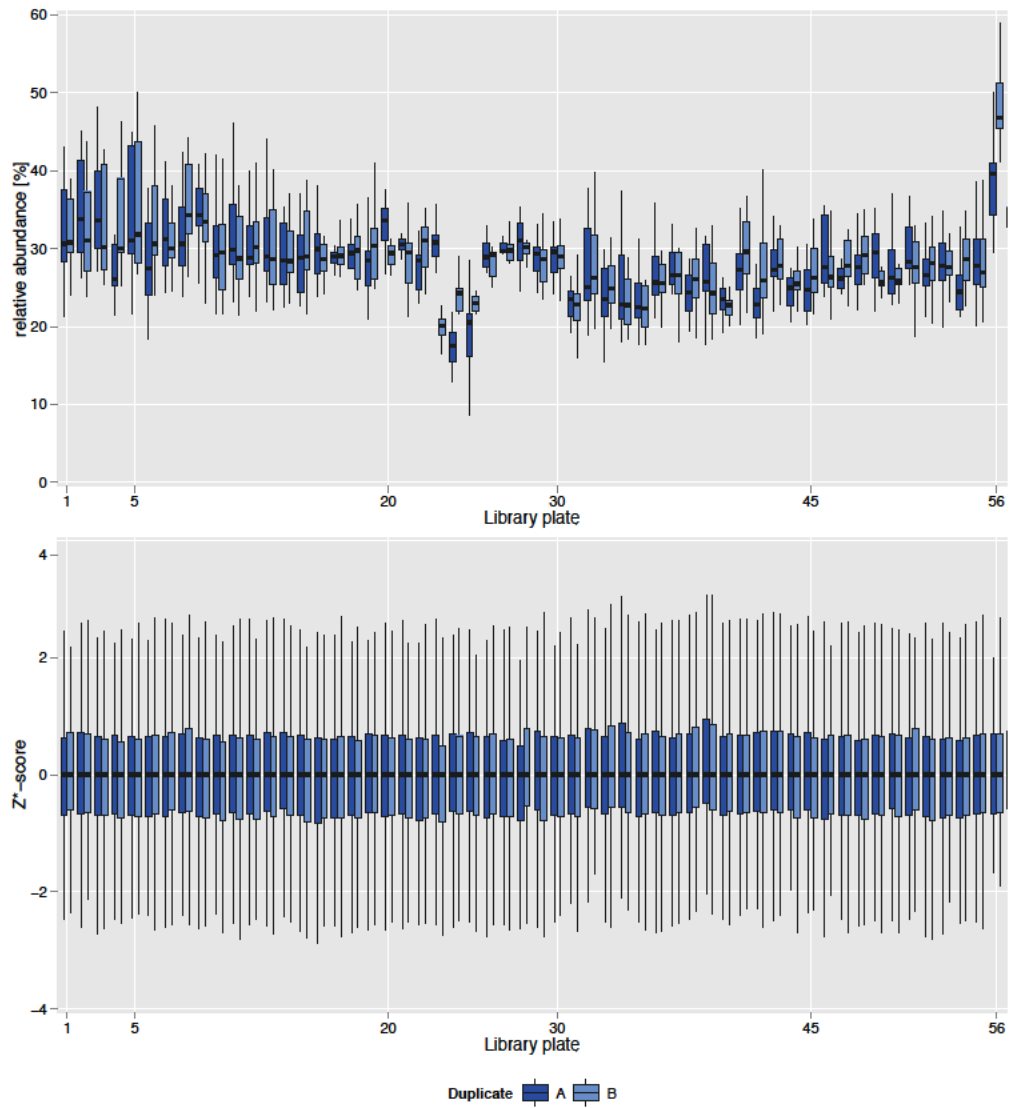


Figure 13: Z*-score transformation archives interplate normalization

A boxplot of the relative abundance of the cell cycle class 8CG2 (top panel) visualizes the plate-to-plate variation in the primary screen, which is normalized after Z*-score transformation shown by a boxplot of the corresponding Z*-score values (bottom panel).

2. RESULTS

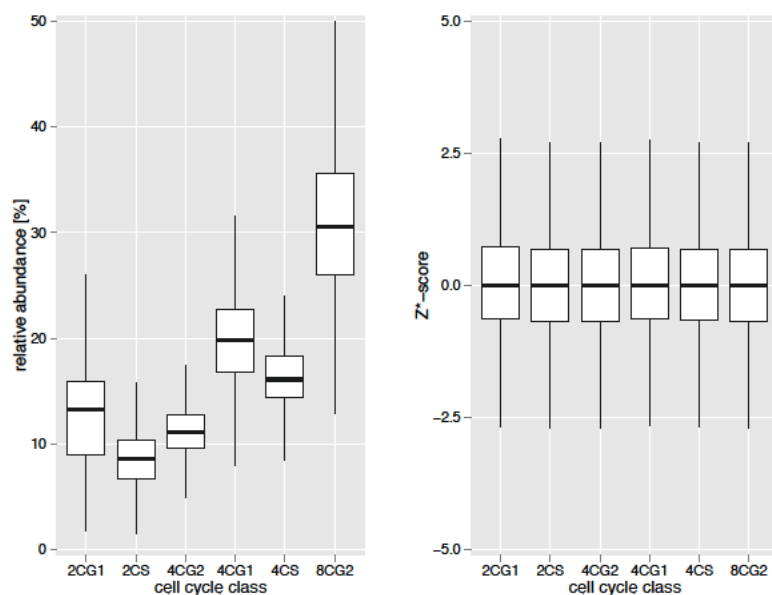


Figure 14: Cell cycle classes have a isotropic variance after Z^* -score transformation

The boxplot in the left panel shows that relative abundance of the 6 different cycle classes as well as their variance differ, which is normalized after the Z^* -score transformation shown by the boxplot of the corresponding Z^* -score values in the right panel.

2.3.3 Selection of primary hits

To determine which cell cycle class is most relevant for identification of genes that affect the proliferation of tetraploid cells, we first quantified the effect from the controls, using as follows: 4 wells containing esiRNA against TP53, 4 wells containing esiRNA against KIFC1 as well as the average of 4 plate quadrants (Q.avg) (figure plate layout, the Q.avg giving the negative control response). To identify the hits, we chose the four cell cycle classes, 2CG1, 4CG2, 4CG1 and 8CG2, which showed the largest separation between TP53 and KIFC1 controls and Q.avg, as well as from the mock conditions not treated with esiRNA (empty) (Figure 15, left panel). We tested several machine learning techniques that use the information of the controls and Q.avg to identify hits (data not shown). Due to the highly heterogeneous behavior of the controls across the whole primary screen (see the paragraph 2.3.5 - “The impact of the SSMD of TP53 controls on the number of

2. RESULTS

primary hits”), we decided to calculate a metric we called Z-index and perform the hit selection independent from the controls. The Z-index is sum of the Z*-scores of % 4CG2 and % 8CG2, from which the Z*-scores of % 2CG1 and % 4CG1 are subtracted, thus we are analyzing the proliferation of tetraploid cells as well as their abundance relative to the diploid cells (Figure 15, right panel). A standard way to determine hits in a high-throughput screen is to consider candidates as hits if their readout value is k standard deviations bigger than the mean off all samples, or k median absolute deviations (MAD) bigger than the median of all samples (Goktug et al., 2013). In accordance with the concept of the Euclidean distance, the separation power of a multivariate-derived value can be compared to a single scalar value by dividing the multivariate-derived value by the square root of the number of variables used to calculate it. Since the Z-index is calculated from 4 isotropic variables, a standard value of 3 MAD corresponds to a Z-index value of 6.

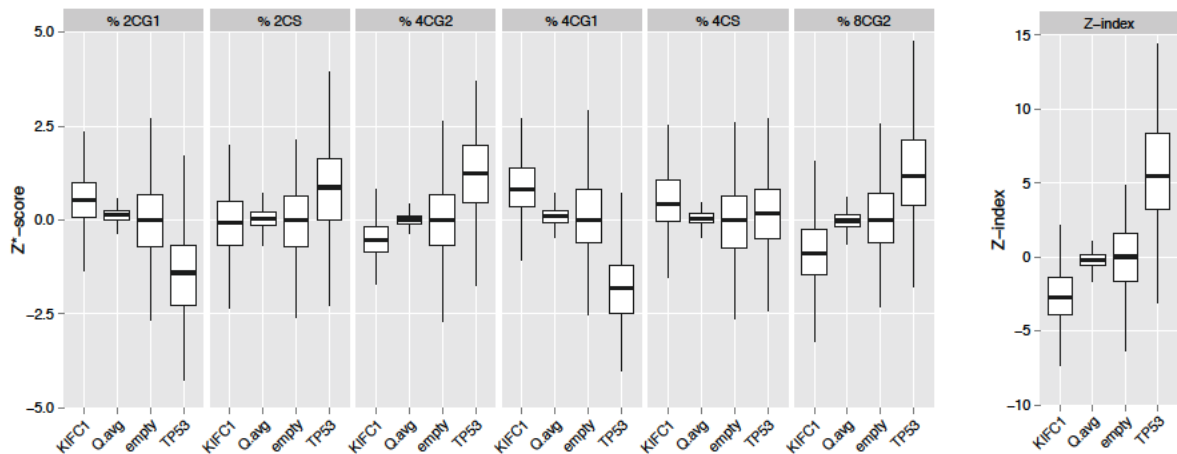


Figure 15: Z*-scores of the relative abundance of the cell cycle classes and the derived Z-index

The boxplots on the left show the Z*-score-transformed relative abundance from the 6 defined cell cycle classes for wells transfected with KIFC1, without RNAi (empty), or TP53 targeting esiRNA; as well as the average of all wells in one quarter of the plate without the control wells. On the right the boxplot of the Z-index, which is the sum of the Z*-scores of % 4CG2 and % 8CG2 after subtraction of the Z*-scores of % 2CG1 and % 4CG1 for wells transfected with KIFC1, without RNA (empty) or TP53 targeting esiRNA, as well as the average of all wells in one quarter of the plate without the control wells.

2. RESULTS

After inspecting the Z-index values of selected candidates that either have a function in the G₁/S transition or have been reported to be involved in the arrest of tetraploid cells, such as RB1 or CDKN1A (p21) (Table 1) (Andreassen et al., 2001), the cutoff for candidates to score as a primary hit was set to 5.875. The primary screen was conducted in two technical replicates, thus the duplicate information can either be used to reduce the false positive or false negative discovery rate. We decided to use the duplicate information to minimize the false negative discovery rate, because false positive hits can easily be eliminated in subsequent confirmatory screens, if the total number of hits is not too big as in our case.

Gene name	Protein name	Expected phenotype	Z*-score of cell number		Z-index	
			Dupl. A	Dupl. B	Dupl. A	Dupl. B
CCND1	CycD1	KIFC1-like	-0,724	-0,701	-14,882	-15,340
CDK4	Cdk4	KIFC1-like	-0,862	0,611	-7,542	-4,994
CDKN1A	p21	TP53-like	0,066	0,228	8,433	6,955
KIF11	Eg5	Viability	-2,762	-2,826	0,161	-1,972
MDM2	Mdm2	KIFC1-like	0,681	0,667	-6,991	-5,568
MYC	Myc	KIFC1-like	2,183	1,132	-11,318	-9,793
PLK1	Plk1	Viability	-1,371	-2,869	2,401	-5,391
RB1	Rb	TP53-like	-0,005	0,492	5,879	1,638

Table 1: Selected candidates from literature

Table of genes and corresponding proteins used to set cutoffs due to their anticipated roles (expected phenotypes column). Genes that reduce the cell viability in general were classified as Viability, genes that have a negative impact on cell proliferation after tetraploidization were classified as KIFC1-like, genes that have a positive impact on cell proliferation after tetraploidization were classified as TP53-like. Z*-score of cell number: number of detected cells in the well normalized to plate average. Z-index: as explained in Figure 15.

To eliminate genes that have a major negative impact on the proliferation of cells or cause a mitotic arrest regardless of their ploidy, we did not analyze conditions with the “Viability” phenotype. Genes were classified as a viability hit if one of the duplicates showed a value less than -2 of Z*-score of the number of cells, which means that the total cell number was reduced independent of the DNA content of the cells (Z*-score of cell number). Applying this parameter confirmed the classification as Viability hit for the genes KIF11 and PLK1, both of whose depletions are regularly

2. RESULTS

used as viability controls (Hoffman et al., 2010; Theis and Buchholz, 2011; Zhang, 2011; Casanova et al., 2012; Vainio et al., 2012; Fawdar et al., 2013) (Table 1). Using the above described strategy, we identified 249 genes that reduce the viability in general (viability hits), 1150 genes that inhibition specifically reduces the proliferation of tetraploid cells (KIFC1-like hits) and 432 genes that inhibition specifically increases the proliferation of tetraploid (TP53-like hits) out of the 16231 genes tested in the primary screen.

2.3.4 Effective reproducibility between the duplicate runs of the primary screen

To assess the technical reproducibility of the screen, we used the four Z^* -score values of cell cycle classes, corrected Z^* -score of the number of cells alive and the Z -index of each well to test the intraclass correlation of the duplicates as a measure of how well the duplicates match. The median intraclass correlation coefficient of 34 of 56 library plates was between 0.6 and 0.75, which is considered as a good match, and all remaining 22 library plates had a median between 0.4 and 0.6, which is still considered as a moderate match (Fleiss, 2011) (Figure 16). In total, over 70 % of all wells matched with their duplicate moderately, well or excellently (Fleiss, 2011). Thus, we concluded that the technical reproducibility was sufficient throughout the primary screen.

2. RESULTS

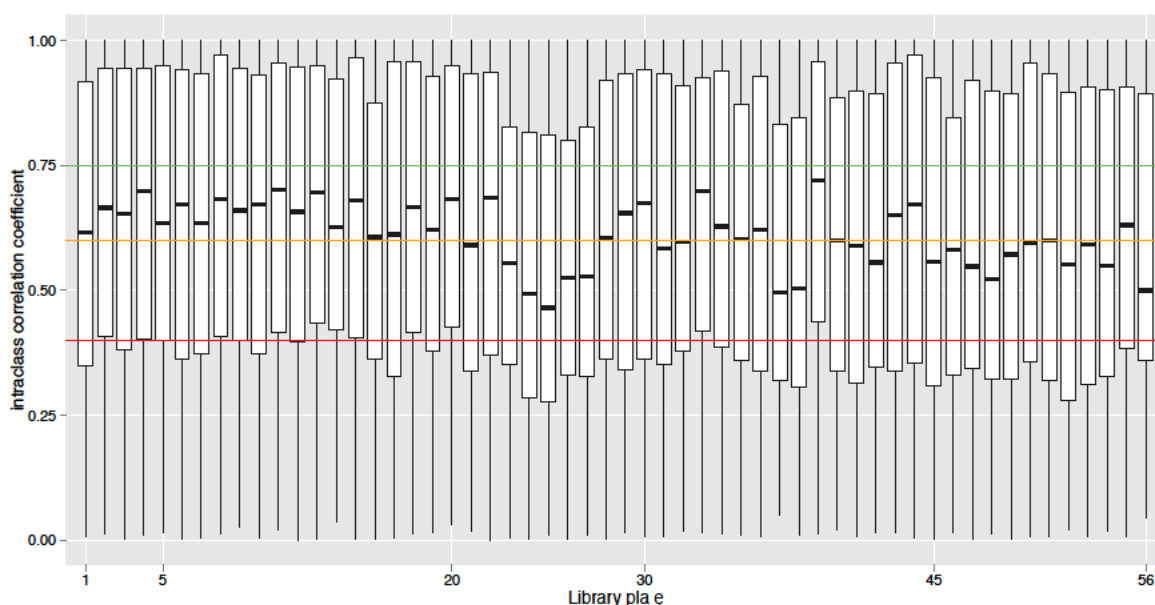


Figure 16: Intra-class correlation between the duplicates

The intra-class correlation for the four different Z^* -score values of the cell cycle classes; the corrected Z^* -score value of the number of cells alive and the Z -index of each well with its duplicate is plotted for each library plate. The red, orange and green lines represent the boundaries between the quality classes, excellent, good, moderate and poor (top to bottom).

2.3.5 The impact of the SSMD of TP53 controls on the number of primary hits

A second common quality control for high-throughput data is to monitor the separation of the positive and negative controls. For this, the strictly standardized mean difference (SSMD) is a common metric. We calculated the robust version of the SSMD, so called SSMD*, for each assay plate. The robust version was chosen due to the low number of wells that could be used to spike in the controls. The SSMD* is the median of Q.avg subtracted from the median of the TP53 control wells divided by the square root of the sum of squared MAD of the controls (Zhang, 2011). In contrast to an intra-class correlation, SSMD* is highly heterogeneous throughout the primary screen. In batch 1, 7 out of 10 plates had SSMD* values above 7, and 2 of the remaining 3 plates with values above 5, these scores are considered excellent or good, respectively. In screens with only one technical replicate, plates with an

2. RESULTS

SSMD value beneath 5 are usually repeated (Zhang, 2011). In batch 2, on average only 1 of the duplicates had a SSMD* above 5, and in batches 3, 4 and 5, on average 0.3, 0.5 and 0.7 plates of each duplicate had a SSMD* above 5, respectively (Figure 17, top panel). Thus, we concluded that the assay itself has a very good dynamic range in general, but problems with the cell transfection or the spiked-in controls occurred in session 3 to 5 and to some degree also in session 2, limiting the robustness of any conclusions. A repetition of all 69 plates with a SSMD* value beneath 5 would mean a tremendous time and financial effort; therefore, we addressed the question whether the bad SSMD* values arose only due to variation in the manually added (spiked-in) controls or whether the whole plates were affected and therefore have to be repeated or disregarded. An insufficient cell transfection is the most likely scenario that affects whole plates and not only the spiked-in controls. In this case the cells would not be affected by the applied esiRNAs. Moreover, because the hit selection based on Z-index is independent from the positive controls, we would expect that the number of identified hits per plate to be decreased along with the SSMD*. Hence, we examined the number of identified primary TP53-like hits per library plate against the SSMD* of its 2 duplicates.

We did not observe any dependency of the number of primary hits per library plate on SSMD*, neither for library plates with only 1 good SSMD* value nor with 2 good SSMD* values (Figure 17, bottom left panel). Moreover, we only observed a non-relevant difference in the number of identified primary TP53-like hits between library plates with at least one duplicate with a SSMD* bigger than 5 and library plates with a SSMD* smaller than 5 in both duplicates (Figure 17, bottom right panel). Together, this data indicate that the poor SSMD* values most likely arose from the variation in the spiked-in controls, rather than problems across the whole assay plate.

2. RESULTS

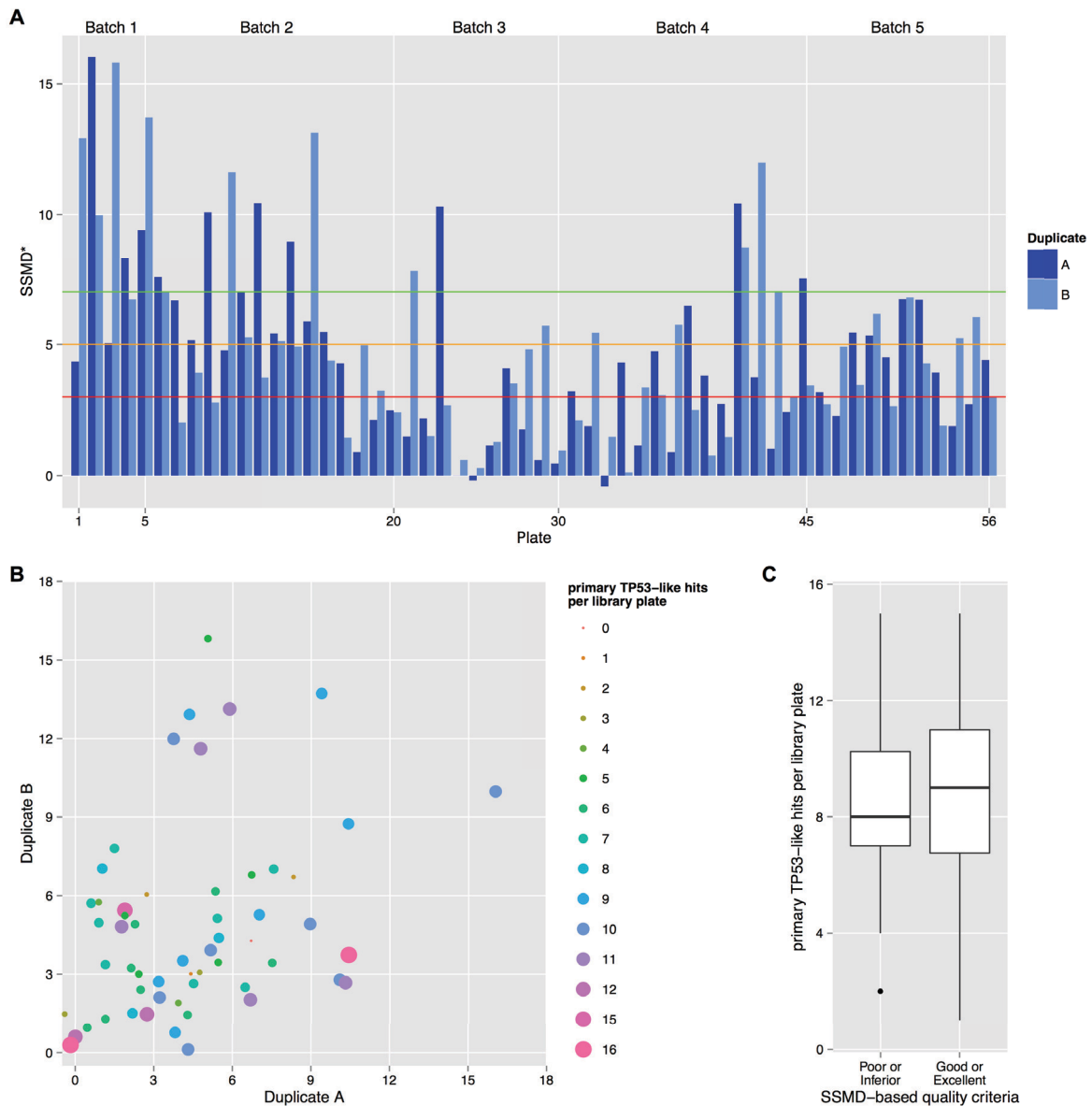


Figure 17: SSMD and its impact on the number of TP53-like hits per library plate

A: The SSMD of each plate of the primary screen. The cutoffs of the SSMD-based quality classes poor, inferior, good and excellent at 3, 5 and 7 are highlighted using a red, orange or a green line, respectively. B: A scatter plot visualized the number of primary TP53-like hits of each library plate encoded by the size and color of the dots versus the SSMD values of duplicate A and B. C: The boxplot support by a violin plot visualizes the distribution of the number of TP53-like hits per library plate for three different quality classes based on the best SSMD of each duplicate.

Therefore, we moved forward and subjected a subset of 374 genes to a confirmatory screen. This subset consists of TP53-like hits identified in the primary screen, but excludes 58 genes that either were identified as hits in previous cell cycle screens (Neumann et al., 2006; Kittler et al., 2007), or are located on the Y chromosome

(which is not present in HCT116 cells), or other genes that did not rationally fit with known biology pathways.

2.3.6 The confirmatory screen of primary TP53-like hits endorses the quality of the primary screen

The confirmatory screen was performed in black 96-well glass bottom plates in four technical replicates. The assumption that most genes tested are not involved in the tested biological process is no longer valid for a confirmatory screen, therefore every assay plate contained four wells of renilla luciferase (R-LUC) and another 4 wells targeting TP53, as negative and positive controls, respectively. As negative controls, the R-Luc wells were used for the Z*-score transformations. The TP53 wells (positive controls) separated well from the R-LUC wells; 56 out of 60 TP53 wells had a Z-index above 5.875 and the Z-index of the R-LUC controls was between -5.875 and 5.875 for 71 out of 72 wells, for one R-LUC well the Z-index was -6.252 (Figure 18 left panel). The separation between the controls was considerably better than in the primary screen (compare Figure 15, right panel). Moreover, the replicates for each tested gene showed mainly excellent intraclass correlation coefficients (Figure 18 right panel). Thus, we concluded that the quality of the confirmatory screen is well suited to confidently reinforce or exclude primary TP53-like hits, as well as to evaluate the quality of the primary screen. To confirm the primary TP53-like hits, every rescreened gene was tested against the R-LUC controls using the Dunnett's multiple comparison test; we considered a primary hit as confirmed if the p-value was less than 0.1. Using this approach, 157 genes out of 373 primary hits were confirmed as TP53-like hits; and furthermore, 6 KIFC1-like hits were identified.

2. RESULTS

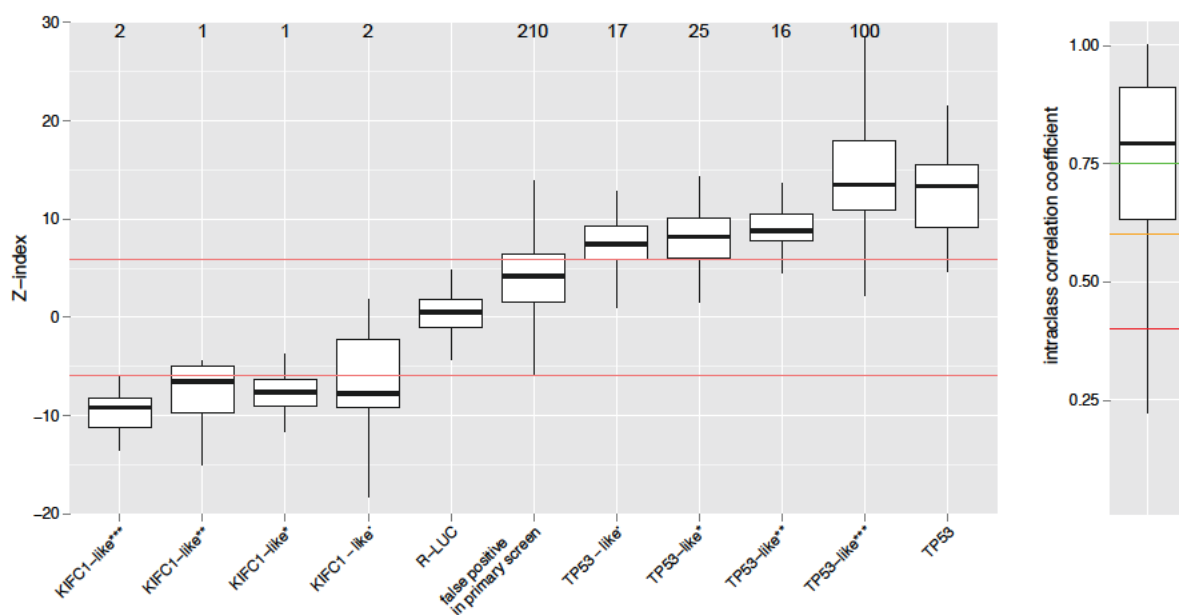


Figure 18: Results and quality of TP53 confirmatory screen

Left panel: Boxplot of Z-index of the confirmed hit classes and the controls R-LUC and TP53. The numbers above indicate the number of genes within the respective class. The horizontal red lines mark the cutoff of the primary screen. Right panel: A boxplot of the intraclass correlation coefficient of the 4 Z*-score values of the cell cycle classes and the Z-index for the 4 replicates is plotted. The red, orange and green lines represent the boundaries between the quality classes, excellent, good, moderate and poor (top to bottom).

To assess the cutoff threshold of the primary screen, we ask at what median Z-index the probability to affect the proliferation of tetraploid cells began to increase. The cutoff of 5.875 (indicated by the red lines) coincides well with the median Z-indices of genes with p-values between 0.90 and 0.45 (Figure 19) and the total confirmation rate of 42 % further indicates that the cutoff is neither too permissive nor too stringent.

The confirmation rate of high throughput screens is another commonly used quality metric (Gribbon et al., 2005). Therefore, we calculated the confirmation rates for each batch and observed values between 25 % and 57 %, which is in the normal range for high throughput data. Furthermore, in agreement with previous high throughput data, we observed a clear correlation ($R^2 = 0.83$) between the median SSMD* of a batch and its related confirmation rate of TP53-like hits, as previously described (Gribbon et al., 2005).

2. RESULTS

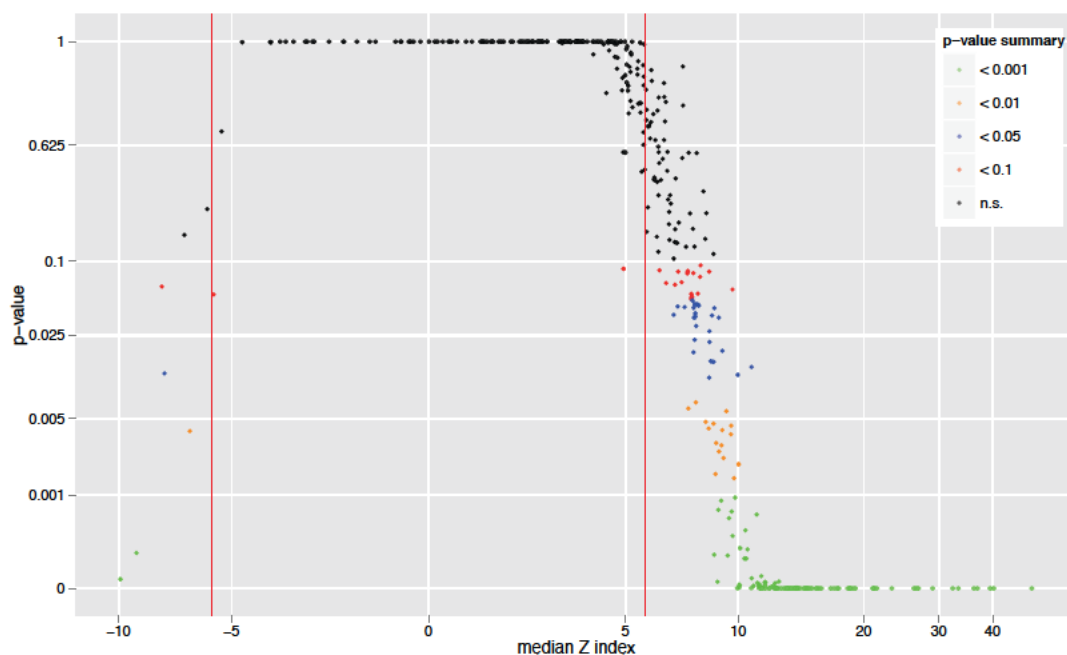


Figure 19: The effect of the Z-index on the statistical probability to affect the 4N proliferation

The p-value of the Dunnett's multiple comparison test of each rescreened gene plotted against its median Z-index. The p-value is plotted on a log-scale and the median Z-index on a generalized log-scale (Ames, 1983; Shibutani et al., 1991; Trotter, 2007). The color of the dots encode the different class of the p-value; genes with not significant (n.s.) p-values are plotted in black, genes with a p-value < 0.1 in red, < 0.05 in blue, < 0.01 in orange, and < 0.001 in green.

However, our ultimate interest is to determine whether the number of false negatives is unacceptably increased in the batches with a median SSMD* smaller than five. Since this value is not directly accessible, we used the number of primary and confirmed hits as an indirect metric. We did not observe any correlation between the median SSMD* and number of genes that were identified as a primary hit or confirmed as TP53-like hit (Table 2).

Thus, we concluded that the commonly used quality cutoffs for metrics monitoring the separation of the positive and negative controls might be too stringent if duplicates are used to minimize the number of false negatives.

2. RESULTS

Batch	no. of library plates	median SSMD*	avg. primary TP53- & KIFC1-like hits per library plate	avg. confirmed TP53-like hits per library plate	confirmation rate of TP53-like hits
1	5	9.7	33.2	4.0	57 %
2	15	5.0	20.6	2.8	41 %
3	10	1.5	48.4	3.9	31 %
4	15	3.1	16.7	1.3	25 %
5	10.13*	4.3	36.8	3.7	42 %

Table 2: Quality control summary

* The last library plate of session 5 (no. 56) only contained esiRNAs targetting 40 instead of 300 genes.

Taken together, we believe that the primary screen as well as the confirmatory screen of primary TP53-like hits were successful and have identified a reasonable number of hits of sufficient quality that grant further analysis.

2.3.7 The pathway analysis of the confirmed TP53-like hits

To gain insight into the biological functions that regulate proliferation of tetraploids, we used public databases such as the Kyoto Encyclopedia of Genes and Genomes (KEGG), Gene Ontology (GO), or Panther database for analysis (Ramanan et al., 2012). We used the Database for Annotation, Visualization and Integrated Discovery (DAVID, (Huang et al., 2009a; 2009b)) online tool to perform an enrichment analysis of GO biological processes (GOBP), KEGG and Panther pathways. No Panther annotated pathway was statistically significantly enriched among the TP53-like hits and the analysis of the KEGG database revealed that the annotation 'Pathways in cancer' was the only one statistically significantly enriched in our data set. Additionally, each of the 4 TP53-like hits from our data set was statistically significantly enriched to a level of about 4-fold in the 'cell cycle arrest' and 'Wnt receptor signaling pathway' clusters in the GOBP analysis.

2. RESULTS

Term	no. of TP53-like hits	EASE p-value	Fold Enrichment
KEGG			
Pathways in cancer	7	0.042	2.6
GOBP			
cell cycle arrest	4	0.060	4.5
Wnt receptor signaling pathway	4	0.078	4.0
negative regulation of nucleobase, nucleoside, nucleotide and nucleic acid metabolic process	10	0.022	2.4
negative regulation of nitrogen compound metabolic process	10	0.024	2.4
negative regulation of cellular metabolic process	14	0.006	2.3
positive regulation of cell proliferation	8	0.058	2.3
negative regulation of transcription	8	0.076	2.1
negative regulation of metabolic process	14	0.012	2.1
negative regulation of macromolecule metabolic process	13	0.019	2.1
DNA metabolic process	9	0.068	2.1
negative regulation of macromolecule biosynthetic process	9	0.077	2.0
negative regulation of cellular biosynthetic process	9	0.085	2.0
negative regulation of biosynthetic process	9	0.095	1.9
negative regulation of cellular process	21	0.055	1.5
negative regulation of biological process	22	0.074	1.4
positive regulation of cellular process	22	0.088	1.4
regulation of nitrogen compound metabolic process	29	0.084	1.3
regulation of cellular metabolic process	35	0.080	1.3
regulation of macromolecule metabolic process	33	0.092	1.3
regulation of primary metabolic process	33	0.099	1.3
regulation of metabolic process	36	0.094	1.3
cellular macromolecule metabolic process	52	0.076	1.2

Table 3: Results of the enrichment analysis of GOBP and KEGG.

EASE is a modified Fisher-Exact test, enrichment above the EASE p-value threshold 0.1 was used as a cutoff.

Moreover, there was a statistically significant enrichment for annotations of metabolic processes that relate to DNA replication (Table 3). This finding is further supported by the functional annotation clustering analysis, which revealed the ‘Wnt signaling pathway’ and ‘DNA replication’ to be among the top 4 clusters (Table 4).

2. RESULTS

		no. of TP53-like hits	EASE p-value	Fold Enrichment
Wnt signaling pathway	Enrichment Score: 0.71			
GOBP	Wnt receptor signaling pathway	4	0.078	4.0
KEGG pathway	Wnt signaling pathway	3	0.303	2.7
PANTHER pathway	Wnt signaling pathway	5	0.306	1.7
DNA replication	Enrichment Score: 0.71			
KEGG pathway	DNA replication	3	0.040	9.2
KEGG pathway	Pyrimidine metabolism	3	0.195	3.6
KEGG pathway	Purine metabolism	3	0.372	2.3
GOBP	DNA replication	3	0.497	1.8

Table 4: Summary of the functional annotation clustering of Wnt signaling pathway and DNA replication

Thus, the bioinformatics analysis using DAVID suggests that the pathways ‘Pathways in cancer’, ‘Wnt signaling pathway’ and ‘DNA replication’, as well as pathways that relate to the DNA metabolism such as ‘DNA metabolic process’ or ‘negative regulation of nucleobase, nucleoside, nucleotide and nucleic acid metabolic process’ for example, might play a key role for the cell proliferation after tetraploidization; the genes annotated in the these pathways are summarized in Table 5.

Pathway	Gene name
Pathways in cancer	GLI1, HSP90AB1, FGFR2, JAK1, CCDC6, LAMC2, CDKN1A
Wnt signaling pathway	SFRP2, GSK3A, DACT2, HMGXB4, TBL1XR1, BTRC
DNA replication	POLA1, POLA2, PRIM1

Table 5: Genes annotated by DAVID in the three identified pathways

2.3.8 Canonical Wnt signaling might support the proliferation after tetraploidization

According to the DAVID pathway analysis, the confirmed TP53-like hits were significantly enriched in the Wnt signaling pathway. Hence, we mapped the confirmed TP53-like and the primary KIFC1-like hits on a simplified but up-to-date model of Wnt signaling pathway (Clevers and Nusse, 2012).

2. RESULTS

This revealed that the negative regulators of Wnt signaling sFRP2, GSK-3 α , β -TrCP were identified as confirmed TP53-like hits (Hart et al., 1999; Liu et al., 1999; Asuni et al., 2006; Doble et al., 2007; Anastas and Moon, 2013).

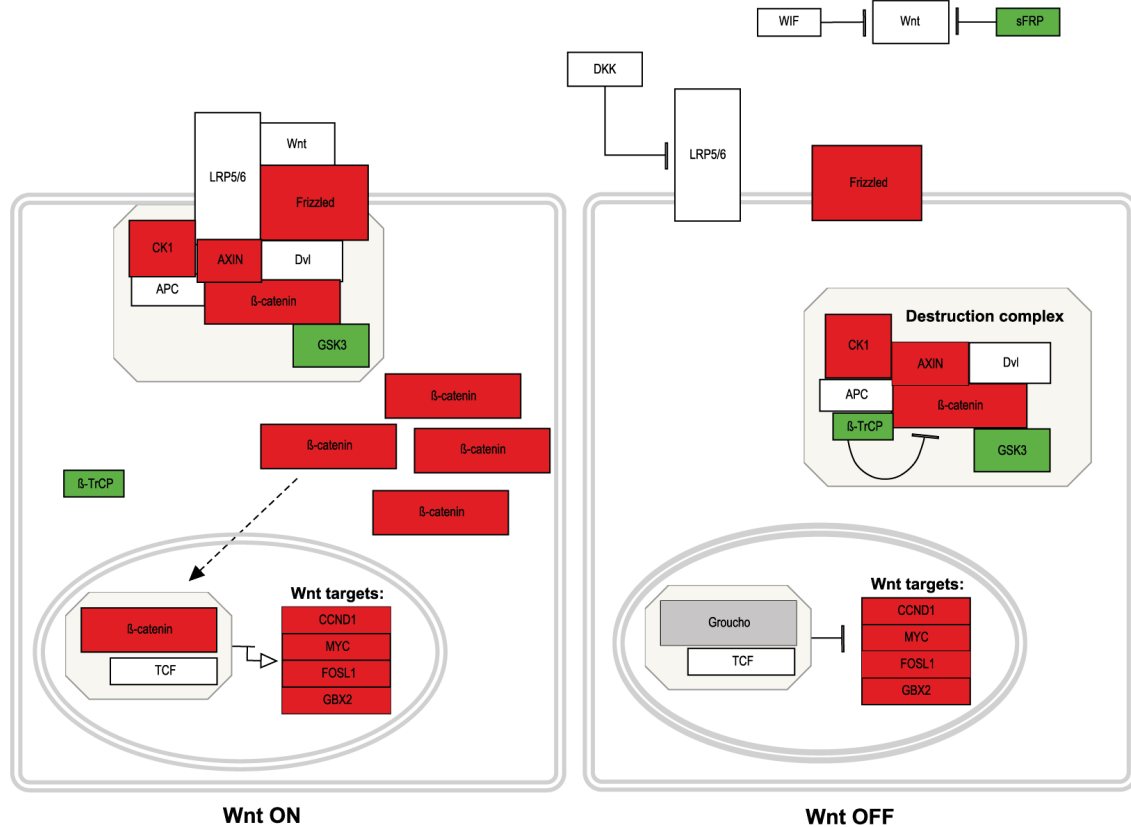


Figure 20: Several core components of the canonical Wnt signaling pathway were identified as primary KIFC1-like hits or confirmed TP53-like hits

The confirmed TP53-like and the primary KIFC1-like hits were mapped on a current simplified model of the β -catenin-dependent Wnt signaling pathway. Frizzled receptor and LRP5 or LRP6 binding Wnt sequesters the destruction complex, which consists of Axin, APC, Dvl, the kinases CK1 and GSK3 and β -catenin. Sequestered destruction complexes are inactive and cannot degrade the bound β -catenin. Therefore, β -catenin accumulates and shuttles into the nucleus, where it activates TCF transcription factors and drives the expression of Wnt target genes like MYC, FOSL1 or GBX2. If sFRP proteins or WIF inhibits the Wnt signal, or DKK proteins inhibit LRP5/6, the destruction complex resides in cytoplasm and degrades β -catenin via β -TrCP. Thus, without the accumulation of cytoplasmic β -catenin the TCF transcription factors repress the expression of Wnt target genes. Confirmed TP53-like hits are represented on a green background; KIFC1-like hits on a red background. Genes represented on a white background were either not identified in the primary screen or were identified as false positives in the confirmatory screen.

Furthermore, additional components were identified as KIFC1-like hits from the primary screen, including: FZD2 that encodes a Frizzled receptors, AXIN1, which is part of the destruction complex and is required to initiate Wnt signaling, CSNK1A1L

2. RESULTS

encoding a member of the casein kinase 1 family and β -catenin (Clevers and Nusse, 2012).

Moreover, 4 Wnt target genes, CCND1 (Cyclin D1) (Shtutman et al., 1999; Tetsu and McCormick, 1999), MYC (He, 1998), FOSL1 (Mann et al., 1999) and GBX2 (Li et al., 2009) were also identified as KIFC1-like hits in the primary screen (Figure 20). Together, these results assemble a picture where the knockdowns of negative regulators promote, and positive regulators impair, the proliferation after tetraploidization.

2.3.9 Meta-analysis of the ‘Project Achilles’ and the identified primary KIFC1-like hits reveal common vulnerabilities of cells CIN

Chromosomal unstable cancers relapse frequently, probably due to their heterogenic cell population and intrinsic multidrug resistances (Lee et al., 2011). Hence, one could hypothesize that genes that are not only essential for tumors that have evolved from tetraploid cells, but also for cells just after tetraploidization would be ideal targets for the treatment of CIN cancer (Shackney et al., 1989; Ganem et al., 2009; Pellman, 2007; Storchova and Kuffer, 2008). We therefore attempted to identify these genes using four steps: First, we selected suitable cancer types that are frequently hypertriploid or hypotetraploid and chromosomally unstable. Second, we identified genes that are essential for the majority of cell lines from a chosen cancer type. Third, the genes that are only essential for a specific cancer type were filtered out, and finally, only genes were retained that had a selective negative effect on the proliferation of cells after tetraploization.

To this end, we analyzed data from the ‘Project Achilles’, which provides genome-wide data on cell proliferation from pooled-shRNA screens from 102 cancer

2. RESULTS

cell lines (Cheung et al., 2011). We used the data from pancreatic, colorectal and ovarian cancer cell lines, as these are frequently hypertriploid or hypotetraploid and chromosomal unstable, unlike hematological malignancies such as leukemia (Figure 21). In a second step, for each cancer type we selected genes where at least two shRNAs produced a decreased abundance by more than double the median absolute deviations (PMAD less than -2) in the majority of the tested cancer cell lines (Figure 22 top panel).

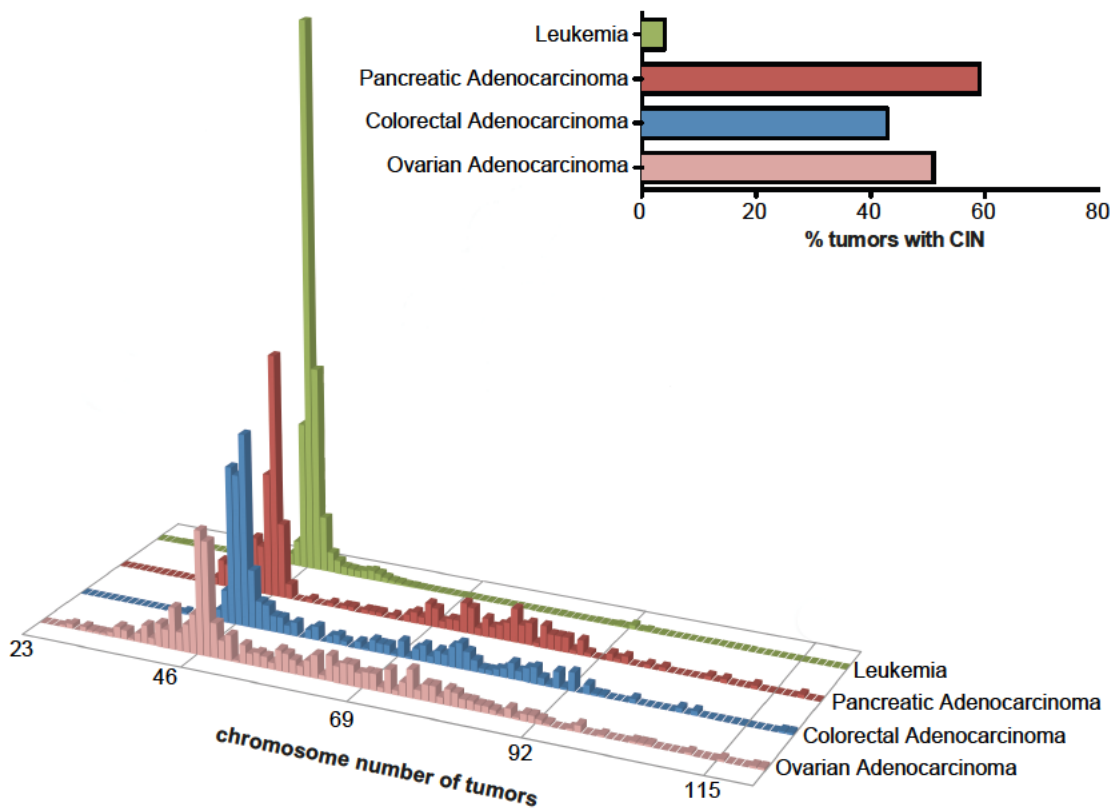


Figure 21: Aneuploidy and CIN in ovarian, colorectal and pancreatic cancer

Chromosomal instability and chromosome number distribution for the selected cancer types in comparison to leukemia, which is usually diploid and chromosomally stable. Top right: Barplot showing the percentage of tumors with CIN (deviating chromosome counts). Bottom: Distribution of the tumor chromosome counts for the selected cancer types. The Mitelman Database of Chromosome Aberrations in Cancers (<http://cgap.nci.nih.gov/Chromosomes/Mitelman>) was used as the source of the data.

2. RESULTS

In the case of colorectal cancer cell line, we used only cell lines that were confirmed to be CIN (Lee et al., 2011). In the third step, we filtered 72 genes that were identified in all three cancer types (Figure 22 bottom panel).

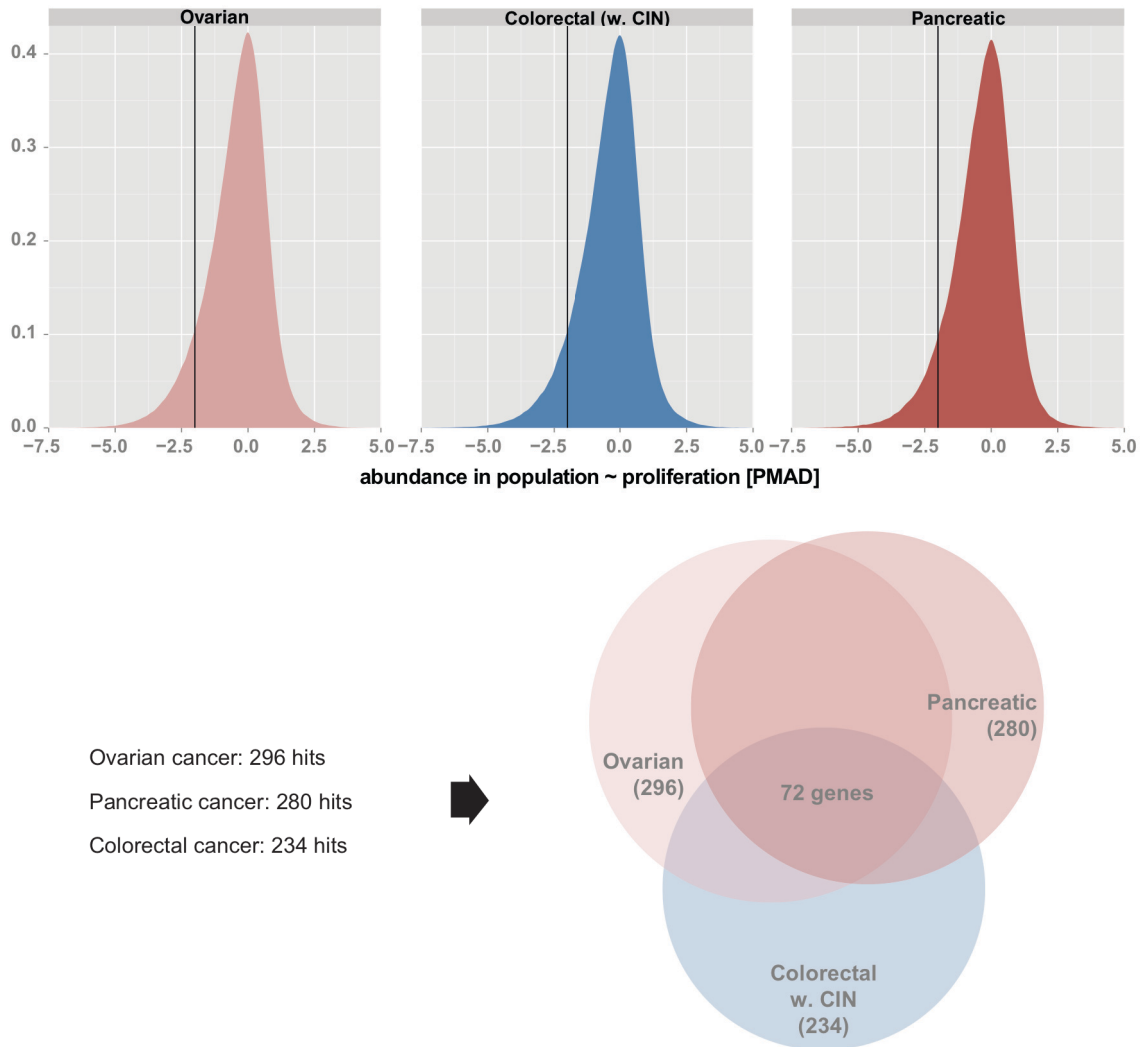


Figure 22: Shared vulnerabilities of frequently CIN cancer types.

Top panel: The density distribution of the median abundance of the shRNAs in the population for the three selected cancer type. Genes were selected as a hit if two independent shRNAs displayed a median below -2 for a given cancer type. The vertical line indicates the PMAD cutoff at -2. Bottom: A Venn Euler diagram illustrates the overlap of the hits for the different cancer types.

All 72 genes that we have identified as essential for CIN cancers have also been included in our screen described above. Combining this data, 18 genes that are essential for CIN cancers were identified to be also essential for cells after tetraploidization (Table 6). KEGG annotation revealed that the identified genes are Proteasome, Ribosome, Spliceosome, RNA transport, mRNA surveillance pathway

2. RESULTS

and Aminoacyl-tRNA biosynthesis; 4 genes have not been annotated to any KEGG pathway.

Gene name	KEGG pathway
PSMA1	Proteasome
PSMA2	Proteasome
PSMB2	Proteasome
PSMB6	Proteasome
RBM8A	RNA transport, mRNA surveillance pathway, Spliceosome
EIF4A3	RNA transport, mRNA surveillance pathway, Spliceosome
PRPF31	Spliceosome
SNRPD2	Spliceosome
NUP93	RNA transport
RPL6	Ribosome
RPL37	Ribosome
RPS3A	Ribosome
RPSA	Ribosome
ARCN1	
DDX21	
ICK	
KARS	Aminoacyl-tRNA biosynthesis
NAPA	

Table 6: Genes essential for both cells after tetraploidization and CIN cancer cell lines.

3. DISCUSSION

Upon tetraploidization mammalian cells become chromosomally unstable (Fujiwara et al., 2005; Ganem et al., 2009; Dewhurst et al., 2014) and may undergo transformation to malignancy (Shackney et al., 1989; Ganem and Pellman, 2007; Storchova and Kuffer, 2008). Untransformed mammalian cells with a functional p53-pathway are able to complete the first cell cycle after tetraploidization (Uetake and Sluder, 2004; Wong and Stearns, 2005), however, their proliferation is limited by the p53 tumor suppressor (Cross et al., 1995; Andreassen et al., 2001; Fujiwara et al., 2005). Thus, it remained enigmatic when and how p53 is activated after tetraploidization and what prevents proliferation and transformation of tetraploid cells given that tetraploid cells can be found in nearly every tissue with relatively high incidence (0.5 – 20%) (Biesterfeld et al., 1994).

3.1 ROS trigger a p53-mediated arrest due to chromosome segregation errors after tetraploidization

The data presented in chapter 2.1.1 (Kuffer et al., 2013) addressed the question, when and how p53 is activated after tetraploidization. Tracking the fate of individual cells by live cell imaging over several days, it shows in agreement with the previous findings that cells with functional p53 that have completed the first cell cycle after tetraploidization frequently arrest in following G1 stage of the cell cycle, while cells without p53 sustain their cell cycle progression. Further, it provides evidence that mitotic abnormalities lead to the p53 accumulation in the trailing interphase and to a cell cycle arrest. A similar result was shown previously for diploid cells, where the missegregation of a single chromosomes also triggered a p53-depedent arrest that prevents the proliferation of aneuploidy cell; the authors showed further that the inhibition of the MAP kinase p38 allows proliferation of aneuploidy cells (Thompson and Compton, 2010). Another report showed that pharmacological prolongation of the prometaphase also leads to an irreversible p38- and p53-dependent arrest in diploid cells (Uetake and Sluder, 2010). The data presented here do support this finding. Even without pharmacological interference, diploid cells whose daughter cells did not proliferate spend in average longer time in mitosis when compared to the case where the daughter cells did proliferate. However, this correlation was not observed for tetraploid cells. Neither the inhibition of p38 by RNAi, nor treatment with chemical inhibitors rescued the cell cycle arrest after tetraploidization. Therefore, it can be concluded that for tetraploid cells the major trigger for the activation of p53-mediated arrest is independent of p38.

Further to this, the SAC component BubR1, and the DNA damage responsive kinases Chk1, Chk2 and ATM were tested, as these candidate genes have been

3. DISCUSSION

implicated in mitotic defects, and/or p53 activation due to mitotic defects (Vitale et al., 2007; Li et al., 2010; Stolz et al., 2010). Among the tested candidates only ATM enhanced the proliferation after tetraploidization. ATM plays a key role as an apical kinase in the repair of DNA double strand breaks (Shiloh and Ziv, 2013); moreover, it was shown that DNA double strand breaks with γ -H2AX accumulated at the break sites can occur due the mitotic failures (Guerrero et al., 2010; Janssen et al., 2011). Thus, the accumulation of γ -H2AX upon tetraploidization was analyzed. First, in contrast to diploid cells treated with a DNA damaging agent, the dynamics of the p53 levels did not follow the dynamics of γ -H2AX upon induction of cytokinesis failures. Second, on single cell level we did not find a correlation between the nuclear level of γ -H2AX and p53. Together, no evidence was found that p53 is activated and cell arrest after tetraploidization due to DNA damage. However, this finding should be interpreted that tetraploid cells do experience an increase of DNA double strand breaks, but the observed levels are not sufficient to significantly diminish the cell proliferation after tetraploidization.

On the other hand, 8-OHdG, an oxidative DNA damage, increased at the same time as p53 accumulated, starting only 24 h after tetraploidization. Further, the nuclear p53 levels also tightly correlated on single cell level with the amount of the oxidative DNA damage 8-OHdG. Previously, it was shown that ROS activate ATM in a non-canonical fashion and lead to ATM-mediated phosphorylation of p53 at Serine 15. Accordingly, the RNAi-mediated knockdown of ATM to decreased p53 and phospho-serine15 p53 after tetraploidization. This finding is in agreement with a study demonstrating that diploid cells with a compromised SAC and high missegregation rates experience elevated ROS levels and ATM suppresses tumorigenesis by stabilizing p53 through phosphorylation of its residue serine15 (Li et

3. DISCUSSION

al., 2010). ROS are considered tumorigenic due to their mutagenic potential (Ames, 1983; Shibutani et al., 1991) and ROS have also been implicated in increased cell proliferation (Pelicano et al., 2004). Additionally, it has been reported that oncogene-induced Nrf2 transcription contributes to tumor development by ROS detoxification (DeNicola et al., 2011) and that tumors evolve only from cells with fine-tuned ROS levels (Perera and Bardeesy, 2011). The presented findings support a pivotal role of ROS during tumorigenesis.

On the other hand, it remains enigmatic how aneuploidy triggers the increase of ROS levels. One possible explanation is provided by the notion that genes involved in physical or genetical interaction have to be kept at similar ratios (Veitia, 2010). Recently it shown that aneuploid cells down regulate 25% of the proteins encoded on extra chromosomes back to the wild type levels. This is most likely mediated by activation of the p62/SQSTM1-mediated selective autophagy and lysosomal pathway (Stingele et al., 2012), pathways that are energy-dependent. Thus, it is not surprising that aneuploid cells have an elevated metabolism (Williams et al., 2008), which might cause the increased ROS levels. Moreover, autophagy is essential for the turnover of mitochondria and the elimination of damaged mitochondria (Lemasters, 2005; Kim et al., 2007; Youle and Narendra, 2011; Kongara and Karantza, 2012), hence, autophagy-deficient cells produce increased ROS levels (Mathew et al., 2009; Kongara et al., 2010). Thus, keeping proteins in physical or genetical interaction at similar ratios via autophagy could impair the elimination of damaged mitochondria and thereby cause an increased production of ROS.

Taken together, the data presented in chapter 2.1.1 (Kuffer, et al. 2013) suggest that ROS trigger the p53-dependent cell cycle arrest after aberrant tetraploid mitosis.

3.2 The effect of Myocardin-related transcription factors A and B on the proliferation tetraploid and chromosomally unstable cells

The results presented in chapter 2.2 (Shaposhnikov et al., 2013) show that the stable depletion of MRTF-A and MRTF-B leads to the outgrowth of aneuploid and tetraploid clones. Despite this, the transient depletion of MRTFs did not cause a detectable increased formation of binucleated tetraploid cells, but an increased number of cells with nuclear buds or micronuclei was observed, which argues for an important role of MRTFs for genome stability. This notion is further supported by the fact that pancreatic tumors, which are usually chromosomally unstable (Storchova and Kuffer, 2008), frequently carry mutations in one or both genes that encode the MRTFs (Cerami et al., 2012; Gao et al., 2013).

Myocardin family proteins including myocardin-related transcription factors A and B (MRTFs) and the closely related myocardin are activated by the MAPK/Erk pathway as well as by Rho-GTPases upon serum stimulation (Posern and Treisman, 2006; Miano et al., 2007). An increasing body of evidence suggests a role of the myocardin family in cell cycle regulation and inhibition of uncontrolled proliferation (Tang et al., 2008; Descot et al., 2009; Kimura et al., 2010). Under normal growth conditions, the MRTFs-depleted cells showed an impaired proliferation accompanied with a significantly shortened G₁ phase and a slightly extended S/G₂ phase. This observation can be explained by the fact that the expression of Cyclin D1 was increased and the expression of the cell cycle inhibitors p27Kip1, p18Ink4c and p19Ink4d were decreased upon MRTFs depletion. Moreover, in the absence of growth factors, MRTFs-depleted cells entered S and G₂ phase more frequently than control-depleted cells. Together, this argues that MRTFs play a key role for a timely cell cycle progression.

3. DISCUSSION

Despite the increased number of cells entering S phase, the cell proliferation of MRTFs-depleted cells did not increase, but the expression level of the cell cycle inhibitor p21 was increased. This might be explained by a report showing that a premature G₁/S transition decreases the cellular nucleotide pools and leads to DNA damage due to replication stress. The arising DNA damage leads to increased transcription of p21 via p53 not only in G₁ but also in S and G₂ phase (compare chapter 1.1.2). Moreover, an increased replication stress could also explain the increase of cells with nuclear buds and micronuclei that were observed after transient MRTFs depletion, as it has been previously reported (Burrell et al., 2013).

Taken together, these results suggest an important but complex role for MRTFs in cell cycle regulation and eventually also in tumorigenesis. Further investigation should clarify the link between MRTFs and the outgrowth tetraploid and chromosomally unstable clones after their stable depletion. A comprehensive analysis of genome and transcriptome of the clones isolated after stable MRTFs depletion of MRTFs should provide valuable insights, which factors play a key role in the tetraploidy-driven tumorigenesis.

3.3 Genome-wide screen for genes that modulate the cell proliferation after tetraploidization

Recently, it was demonstrated that the genetic alterations observed in tumors with CIN could be recapitulated using cell populations established by sorting of spontaneously arising tetraploids from chromosomally stable HCT116 colorectal cancer cells (Dewhurst et al., 2014). Additionally, about 37 % of all tumors have experienced tetraploidization in their development (Zack et al., 2013). Hence, probing the proliferation of HCT116 after tetraploidization provides a novel approach to identify genes that enhance or suppress tetraploidy-driven tumorigenesis. This strategy was deployed for genome-wide screen presented in chapter (2.3).

3.3.1 Setup and quality

To identify genes that enhance or suppress the proliferation after tetraploidization, FUCCI cell cycle probes combined with DNA content cell cycle profiling were used in an image-based assay that examines tetraploid and diploid cells side-by-side. Analyzing cells of interest and control cells side-by-side was shown to significantly improve the analysis of genome-wide screens by reducing technical variability (Krastev et al., 2011). Thus, 249 genes that have strong cytotoxic effects on diploid and tetraploid cells alike could be excluded directly after the primary screen without the need to perform a secondary assay.

Quality control metrics of genome-wide RNAi screens are either not published or only a simple correlation coefficient of technical duplicates is reported (Kittler et al., 2007; Kwon et al., 2008; Neumann et al., 2010; Krastev et al., 2011; Kozik et al., 2012). To ensure an adequate quality throughout the primary screen, two metrics were monitored; the intraclass correlation coefficient, which determines the technical

3. DISCUSSION

reproducibility, and the strictly standardized mean difference (SSMD*) between the quadrant averages for the negative control and TP53 as the positive control, which is a measure for dynamic range of the assay. In contrast to the correlation coefficient, the intraclass correlation can calculate concordance of two or more replicates of multivariant observations. The technical reproducibility was sufficient throughout the primary screen.

The SSMD* was highly heterogeneous throughout the primary screen, ranging from excellent to inferior. The fact that in first batch, 7 out of 10 plates had SSMD* values above 7, argues for a very good dynamic range for the used assay in general. Therefore, the question was addressed whether an insufficient cell transfection affected whole plates or only the spiked-in controls. In the first case the cells would not be affected by the applied esiRNAs. If insufficient cell transfection would affect all wells of the plate, the number of identified hits per plate would decrease along with the SSMD*. Hence, the correlation of number of identified primary TP53-like hits per library plate was examined against the SSMD*; however, the number of primary hits did not depend on SSMD*. This suggests that the poor SSMD* values are most likely due to variation in the spiked-in controls, rather than caused by problems that affected the whole assay plate.

In total the primary screen identified 1582 hits out of the 16231 tested genes; 432 genes that specifically increase the proliferation of tetraploid (TP53-like hits) and 1150 genes that specifically reduce the proliferation of tetraploid cells (KIFC1-like hits). The number of identified genes in the primary screen is comparable to the number of primary hits of published genome-wide RNAi screens (Kittler et al., 2007; Kwon et al., 2008; Neumann et al., 2010; Kozik et al., 2012).

3. DISCUSSION

The confirmation screen affirmed the sufficient quality of the primary screen; the confirmation rate of TP53-like hits in each batch ranges between 25 % and 57 %, which is in the normal range for high throughput data (Gribbon et al., 2005). Furthermore, the cutoff chosen for the primary screen was confirmed to be suitable, because p-values above the cutoff value dropped from 0.90 to 0.45 in the confirmation screen. Moreover, the total confirmation rate of 42 % further indicates that the cutoff was neither too permissive nor too stringent. Taken together, this argues for a sufficient quality of the primary screen.

3.3.2 The TP53-like hit and ATM target CCDC6 might contribute to the arrest after tetraploidization via the activation of 14-3-3 σ

The results presented in chapter 2.1 showed that the DNA damage kinase ATM links the increased reactive oxygen species (ROS) with the activation of p53 (Kuffer et al., 2013). Even though we did not identify ATM as TP53-like hit, we identified CCDC6, a reported downstream target of ATM, as a TP53-like hit with a KEGG annotation 'Pathways in cancer'. The ATM-dependent phosphorylation protects CCDC6 from ubiquitination by the SCF complex, and its subsequent ubiquitin-dependent degradation (JunGang et al., 2012). CCDC6 is a direct binding partner of 14-3-3 σ upon insulin stimulation (Dubois et al., 2009) and is also required to sequester CDC25 to the cytoplasm via 14-3-3 σ after genotoxic stress (Thanasopoulou et al., 2012). Furthermore, 14-3-3 σ has been reported to stall cell cycle progression through CDC25 as well as to directly inhibit CDK1, CDK2 and CDK4 (Laronga et al., 2000). Taken together, CCDC6 might cooperate with 14-3-3 proteins parallel to p53 and p21 downstream of ATM to stop cell cycle progression in

3. DISCUSSION

response to the increased levels of reactive oxygen species (ROS) that accumulate after tetraploidization due to chromosome segregation errors.

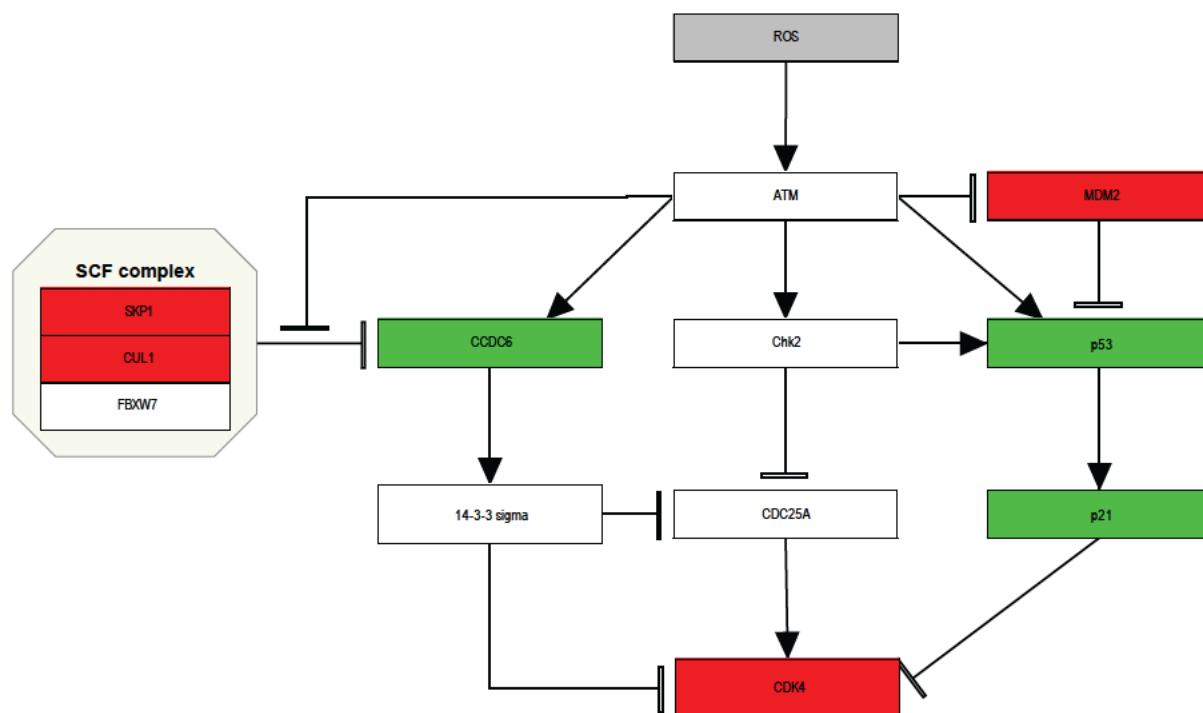


Figure 23: Possible regulatory network mediating the ROS triggered arrest after tetraploidization

TP53-like hits are represented on a green background; KIFC1-like hits on a red background. Genes represented on a white background were either not identified in the primary screen or were identified as false positives in the confirmatory screen. Note: TP53-like hits have been confirmed, while KIFC1-like are primary hits.

3.3.3 Do decreased levels of the DNA polymerase α -primase complex increase the cell proliferation after tetraploidization?

The 'DNA replication' cluster from the DAVID pathway analysis consists of confirmed TP53-like hits POLA1, POLA2 and PRIM1. Their gene products, together with gene product of the primary KIFC1-like hit, PRIM2, constitute the DNA polymerase α -primase complex (pol-prim). During the S-phase, the pol-prim complex synthesizes the initial 8 - 12 nucleotide long RNA primer and extends it by about 20 deoxynucleotides before the DNA proofreading DNA polymerases δ and ϵ

3. DISCUSSION

continue DNA synthesis. Therefore, the function of the pol-prim complex is essential (Loeb and Monnat, 2008) and the yeast knockout homolog of the catalytic subunit of DNA polymerase α is nonviable (Johnson et al., 1985; Giaever et al., 2002) due to an S-phase arrest (Leland H Hartwell, 1973). Thus, the identification of the pol-prim complex might be explained by an immediate S-phase arrest resulting in an increase in binucleated tetraploid cells that do not even enter the first tetraploid mitosis. Despite the fact that a preliminary inspection of raw images did not reveal an elevated number of binucleated cells, a double pulse chase experiment that monitors DNA synthesis using Bromodeoxyuridine (BrdU) and Ethynyldeoxyuridine (EdU) should be conducted as a secondary assay to confirm that the TP53-like phenotype of POLA1, POLA2 and PRIM1 is not an artifact of an S-phase arrest of binucleated cells that resulted in a high Z-index and a systematic false positive classification.

Given that the RNAi-knockdown efficiency differs from gene to gene, and the amount of protein required for its function differs depending on the individual protein, it is likely that the total number of pol-prim complexes was decreased to a level that still allowed the progression through the first cell cycle after tetraploidization. However, the diminished levels of POLA1, POLA2 and PRIM1 may have enriched the relative number of cells in S, G₂ or M phase in the second cell cycle after tetraploidization.

On the other hand, the depletion of the pol-prim nucleotide substrates caused replication stress, genomic instability and increased cell transformation (Bester et al., 2011). Moreover, it was reported that the reduction of fired origins rescued the replication stress phenotype (Jones et al., 2013). Given the essential role of the pol-prim complex in replication initiation, the cell proliferation after tetraploidization might increase after depletion of pol-prim subunits by reducing the number of active replication forks. Together, this suggests a link between un-

3. DISCUSSION

scheduled tetraploidization and genome instability due to the DNA replication stress. Therefore, it will be important to test, first, whether cell experience replication stress after tetraploidization, second whether the knockdown of pol-prim subunits also decreases the replication stress and third, whether the exogenous supply of nucleotides could increase the cell proliferation of tetraploids immediately after tetraploidization.

3.3.4 Wnt signaling activation enhances the proliferation after tetraploidization

The pathway analysis of confirmed TP53-like hits using DAVID identified the Wnt signaling pathway. Aberrant Wnt signaling plays an important role for tumorigenesis of many solid tumors and is intensively studied as potential for anti-cancer therapy (MacDonald et al., 2009; Clevers and Nusse, 2012; Anastas and Moon, 2013). Hence, we mapped the confirmed TP53-like and the primary KIFC1-like hits on a simplified but up-to-date model of Wnt signaling pathway (Clevers and Nusse, 2012). Together, these results assemble a picture where the knockdowns of negative regulators promote, and positive regulators impair the proliferation after tetraploidization. Despite this strong evidence, the results have to be confirmed using an independent assay, for example using a BrdU incorporation assay. Moreover, several questions have to be answered to further elucidate the role of Wnt signaling in proliferation after tetraploidization. First, is an overexpression of β -catenin sufficient to increase the proliferation after tetraploidization or, alternatively, does the expression of available TCF dominant-negative mutants decrease the proliferation after tetraploidization (van de Wetering et al., 2002)? Second, which Frizzled receptors and Wnt ligands are expressed, and which combinations mediate

3. DISCUSSION

a sufficient Wnt signal? Finally, what role does AXIN1 play in the proliferation after tetraploidization, given its role as tumor suppressor in hepatocellular carcinomas, which frequently have near-tetraploid karyotypes (Sato et al., 2000; Storchova and Kuffer, 2008). Answering these questions will help to understand how tetraploidization and β -catenin dependent Wnt signaling interact during tetraploidy-driven tumorigenesis.

3.3.5 Identifying novel anti-cancer drug targets using a meta-analysis of the 'Project Achilles' and the primary KIFC1-like hits

Chromosomally unstable cancers relapse frequently, probably due to their heterogenic cell population and intrinsic multidrug resistances (Lee et al., 2011). Hence, one could hypothesize that the patients with CIN tumors might relapse less often, if during their treatment the factors would be targeted that are essential not only for evolved cancer clones, but also for cells after tetraploidization that initiated tumorigenesis (Shackney et al., 1989; Pellman, 2007; Ganem et al., 2009; Storchova and Kuffer, 2008). Therefore, genes were selected from the primary KIFC1-like hits (gene suppressing cell proliferation after tetraploidization) that showed also a negative effect on the proliferation of cancer cell line with CIN. This selection contained four genes that encode subunits of the 20S proteasome; 74 out of 316 ovarian cancer tumors and 24 out 212 colorectal cancer tumors carry one or more gene amplifications of genes that encode subunits of the 20S proteasome (Cancer Genome Atlas Network, 2011 & 2012; Cerami et al., 2012; Gao et al., 2013). This hints that cells with CIN require an increased proteasome activity and in fact, despite the central cellular function of 20S proteasome, proteasome inhibitors are being developed as anti-cancer drugs, with Bortezomib being the first one approved for the

3. DISCUSSION

clinical use by the Food and Drug Administration (FDA) but they are approved against cancer that is not linked to CIN (Shen et al., 2013).

Moreover, the majority of the identified genes are associated with the KEGG annotations Ribosome, RNA transport, Spliceosome and mRNA surveillance pathway, which are related to the protein translation and its control. The hypothesis that aberrant protein translation contributes to tumorigenesis is currently one of the major ideas of cancer research (Ruggero and Pandolfi, 2003).

Taken together, the present results provide a proof of concept that the designed strategy is capable to identify novel genes that might contribute to tumorigenesis and therefore should be further evaluated as targets for anti-cancer therapy.

3.4 Future directions

In vivo cell transformation and neoplastic growth is strongly influenced by cellular microenvironment, which provides a complex signaling network formed by cell-cell interactions and paracrine signals to maintain tissue homeostasis (De Wever and Mareel, 2003; Hanahan and Weinberg, 2011; Levayer and Moreno, 2013; Wagstaff et al., 2013). The assays chosen to characterize the p53-mediated arrest after tetraploid as well as for the genome-wide screen avoid the isolation of tetraploid cells and therefore the tetraploid proliferation is analyzed in an environment similar to the *in vivo* situation, where the arising tetraploid cells are surrounded by diploid cells. Experimental setups such as presented in this work are likely to provide more physiological relevance than experiments with isolated tetraploid cells. In this context the hits found in the Wnt signaling pathway are particularly interesting, because Wnt signaling has been implied to function in cell competition, a phenomenon that describes the short-range elimination of viable cells by cells with superior fitness (Levayer and Moreno, 2013; Wagstaff et al., 2013). Therefore, future investigations should clarify the role of cell competition in preventing tetraploidy-driven tumorigenesis.

4. MATERIAL & METHODS OF UNPUBLISHED DATA

4.1.1 HCT116 Fucci

HCT116 Fucci was generated in a 2-step protocol. First, FucciG1 cDNA was transfected with FugeneHD (Roche) into HCT116 (ATCC No. CCL-247) according to the manufacturer's protocol. Transfected cells were cultured in selection medium (G418, 500 µg/ml) and after 6 weeks cells were FucciG1 positive cells were sorted using FACS Aria I. Second, HCT116 carrying the FucciG1 construct were transfected with FucciG2 cDNA. Every 10 days cells expressing the FucciG2 construct were selected via FACS.

4.1.2 Experimental procedures of the primary and confirmatory screen

HCT116 Fucci cells were transfected as described previously (Krastev et al., 2011). In brief, 4000 cells were reversely transfected in black 384-well glass-bottom plates (Greiner Bio-One) with 25 ng esiRNA and 0.25 µl Oligofectamine (LifeTechnologies) in 10 µl OptiMem (LifeTechnologies). One day after transfection cells were treated with 0.75 µM Cytochalasin D (DCD, inhibitor of actin polymerization, Sigma) for 18 h. Subsequently the cells were washed 4 times with medium using a BioTek plate washer and placed into a drug-free medium. Cells were fixed with 12 % formaldehyde in PBS (final concentration formaldehyde 4 %) for 20 min followed by 3 PBS washes. Cells were stained with DAPI and stored at 4 °C until image acquisition. Four images per well were acquired using a ScanR screening station (Olympus) equipped with a 10x objective. The number of cells in each cell cycle stage as well as the total cell number of each well was exported with the ScanR analysis software. The primary screen was conducted in 2 replicates and the confirmatory screen in 4 replicates. Each plate of the primary screen contained 4 control wells that positively affected cell proliferation after tetraploidization (esiRNA targeting TP53) and 4 control

wells that negatively affected cell proliferation after tetraploidization (esiRNA targeting KIFC1). For each plate we calculated the average of 4 plate quarters serving as negative controls. In the confirmatory screen, each plate contained 4 positive control wells (esiRNA targeting TP53) and 4 negative control wells (esiRNA targeting renilla luciferase – R-LUC).

4.1.3 Data evaluation and hit selection for the primary screen

For each well the total cell number and the percentage of cells in each cell cycle stage were plate-wise Z-transformed according the formula:

$$z_{i,p} = \frac{x_{i,p} - \widetilde{X}_p}{\widetilde{\sigma}_p}$$

(z: Z-transformed value, \widetilde{X}_p : plate median without control wells, $\widetilde{\sigma}_p$: plate median absolute deviation (MAD) without control wells). The total cell number was corrected with a linear model for systematic errors caused by automatic liquid handling (8-channel dispenser and 96-channel washer) as well as by the edge effect for each batch, using the R correction formula:

```
x ~ Batch / ((as.factor(8-channel dispenser) + as.factor(96-channel washer)) + (I(line^2) * I(column^2)))
```

A viability phenotype was assigned to each esiRNA, if the corrected z-score of total cell number was lower than -2 in any of the technical replicates of the screen.

The Z-index was calculated as sum of the z-scores of 4CG2 and 8CG2 minus the sum of the z-scores of 2CG1 and 4CG1; esiRNAs with Z-indices in any of the two technical replicates above 5.875 were considered as TP53-like hits and esiRNAs with Z-indices below -5.875 were considered as KIFC1-like hits.

4.1.4 Statistical analysis of the confirmatory screen and evaluation of biological pathways

For each well the percentage of cells in each cell cycle stage were plate-wise Z-transformed according the formula:

$$z_{i,p} = \frac{x_{i,p} - \widetilde{X}_{p,RLuc}}{\widetilde{\sigma}_{p,RLuc}}$$

(z: Z-transformed value, $\widetilde{X}_{p,RLuc}$: median of R-Luc control wells from each plate, $\widetilde{\sigma}_{p,RLuc}$: MAD of R-Luc control wells from each plate. The Z-index of each well was calculated as described above. In the confirmatory screen, each esiRNA was compared by an ANOVA-test against R-Luc controls using Dunnett's correction for multiple comparisons. Hits were considered as confirmed for p-values smaller 0.1. The Ensembl gene identifier (ENSG) of the confirmed TP53-like hits was pasted as gene list into the web interface of DAVID as well as the ENSG identifier of all genes tested in the primary screen as background. The pathways were visualized with Pathvisio (van Iersel et al., 2008).

4.1.5 Meta-analysis of KIFC1-like primary hits and 'Project Achilles'

The PMAD normalized 'Project Achilles' data was downloaded from the data portal of the Broad institute (<http://www.broadinstitute.org/achilles>). The data was processed as described above. To merge the data set with the results of our screen converted the EntrezGene identifier to the ENSG identifier by merging with an ENSG EntrezGene lookup table download from Ensembl BioMart web interface (<http://www.ensembl.org/biomart/martview>) first.

4.1.6 Data processing and visualization

All data processing was done using R and Rstudio (R Core Team, 2012; Rstudio, 2013). Data was visualized using the R package ggplot2 (Wickham, 2009).

5. REFERENCES

Abraham, R.T. (2001). Cell cycle checkpoint signaling through the ATM and ATR kinases. *Genes Dev* 15, 2177–2196.

Ames, B.N. (1983). Dietary carcinogens and anticarcinogens. Oxygen radicals and degenerative diseases. *Science* 221, 1256–1264.

Anastas, J.N., and Moon, R.T. (2013). WNT signalling pathways as therapeutic targets in cancer. *Nature Reviews Cancer* 13, 11–26.

Andreassen, P.R., Lohez, O.D., Lacroix, F.B., and Margolis, R.L. (2001). Tetraploid state induces p53-dependent arrest of nontransformed mammalian cells in G1. *Mol Biol Cell* 12, 1315–1328.

Asuni, A.A., Hooper, C., Reynolds, C.H., Lovestone, S., Anderton, B.H., and Killick, R. (2006). GSK3alpha exhibits beta-catenin and tau directed kinase activities that are modulated by Wnt. *Eur. J. Neurosci.* 24, 3387–3392.

Bakkenist, C.J., and Kastan, M.B. (2003). DNA damage activates ATM through intermolecular autophosphorylation and dimer dissociation. *Nature* 421, 499–506.

Barrett, M.T., Pritchard, D., Palanca-Wessels, C., Anderson, J., Reid, B.J., and Rabinovitch, P.S. (2003). Molecular phenotype of spontaneously arising 4N (G2-tetraploid) intermediates of neoplastic progression in Barrett's esophagus. *Cancer Res* 63, 4211–4217.

Bartek, J., and Lukas, J. (2001). Pathways governing G1/S transition and their response to DNA damage. *FEBS Lett.* 490, 117–122.

Bester, A.C., Roniger, M., Oren, Y.S., Im, M.M., Sarni, D., Chaoat, M., Bensimon, A., Zamir, G., Shewach, D.S., and Kerem, B. (2011). Nucleotide deficiency promotes genomic instability in early stages of cancer development. *Cell* 145, 435–446.

Biesterfeld, S., Gerres, K., Fischer-Wein, G., and Böcking, A. (1994). Polyploidy in non-neoplastic tissues. *J Clin Pathol* 47, 38–42.

Brito, D.A., and Rieder, C.L. (2006). Mitotic checkpoint slippage in humans occurs via cyclin B destruction in the presence of an active checkpoint. *Curr Biol* 16, 1194–1200.

Burrell, R.A., McClelland, S.E., Endesfelder, D., Groth, P., Weller, M.-C., Shaikh, N., Domingo, E., Kanu, N., Dewhurst, S.M., Grönroos, E., et al. (2013). Replication stress links structural and numerical cancer chromosomal instability. *Nature* 494, 492–496.

Caldwell, C.M., Green, R.A., and Kaplan, K.B. (2007). APC mutations lead to cytokinetic failures in vitro and tetraploid genotypes in Min mice. *J Cell Biol* 178, 1109–1120.

5. REFERENCES

- Cancer Genome Atlas Network (2012). Comprehensive molecular characterization of human colon and rectal cancer. *Nature* 487, 330–337.
- Cancer Genome Atlas Research Network (2011). Integrated genomic analyses of ovarian carcinoma. *Nature* 474, 609–615.
- Casanova, C.M., Sehr, P., Putzker, K., Hentze, M.W., Neumann, B., Duncan, K.E., and Thoma, C. (2012). Automated high-throughput RNAi screening in human cells combined with reporter mRNA transfection to identify novel regulators of translation. *PLoS ONE* 7, e45943.
- Castillo, A., Morse, H.C., Godfrey, V.L., Naeem, R., and Justice, M.J. (2007). Overexpression of Eg5 causes genomic instability and tumor formation in mice. *Cancer Res* 67, 10138–10147.
- Cerami, E., Gao, J., Dogrusoz, U., Gross, B.E., Sumer, S.O., Aksoy, B.A., Jacobsen, A., Byrne, C.J., Heuer, M.L., Larsson, E., et al. (2012). The cBio Cancer Genomics Portal: An Open Platform for Exploring Multidimensional Cancer Genomics Data. *Cancer Discov* 2, 401–404.
- Cheung, H.W., Cowley, G.S., Weir, B.A., Boehm, J.S., Rusin, S., Scott, J.A., East, A., Ali, L.D., Lizotte, P.H., Wong, T.C., et al. (2011). Systematic investigation of genetic vulnerabilities across cancer cell lines reveals lineage-specific dependencies in ovarian cancer. *Proc Natl Acad Sci USA* 108, 12372–12377.
- Chowdhury, D., Keogh, M.-C., Ishii, H., Peterson, C.L., Buratowski, S., and Lieberman, J. (2005). gamma-H2AX dephosphorylation by protein phosphatase 2A facilitates DNA double-strand break repair. *Mol Cell* 20, 801–809.
- Chowdhury, D., Xu, X., Zhong, X., Ahmed, F., Zhong, J., Liao, J., Dykxhoorn, D.M., Weinstock, D.M., Pfeifer, G.P., and Lieberman, J. (2008). A PP4-phosphatase complex dephosphorylates gamma-H2AX generated during DNA replication. *Mol Cell* 31, 33–46.
- Clevers, H. (2006). Wnt/beta-catenin signaling in development and disease. *Cell* 127, 469–480.
- Clevers, H., and Nusse, R. (2012). Wnt/ β -catenin signaling and disease. *Cell* 149, 1192–1205.
- Crasta, K., Ganem, N.J., Dagher, R., Lantermann, A.B., Ivanova, E.V., Pan, Y., Nezi, L., Protopopov, A., Chowdhury, D., and Pellman, D. (2012). DNA breaks and chromosome pulverization from errors in mitosis. *Nature* –.
- Cross, S.M., Sanchez, C.A., Morgan, C.A., Schimke, M.K., Ramel, S., Idzerda, R.L., Raskind, W.H., and Reid, B.J. (1995). A p53-dependent mouse spindle checkpoint. *Science* 267, 1353–1356.
- Dalton, W.B., Nandan, M.O., Moore, R.T., and Yang, V.W. (2007). Human cancer cells commonly acquire DNA damage during mitotic arrest. *Cancer Res* 67, 11487–11492.
-

5. REFERENCES

- Danes, B.S. (1976). The Gardner syndrome: increased tetraploidy in cultured skin fibroblast. *J. Med. Genet.* 13, 52–56.
- Daniels, M.J., Wang, Y., Lee, M., and Venkitaraman, A.R. (2004). Abnormal cytokinesis in cells deficient in the breast cancer susceptibility protein BRCA2. *Science* 306, 876–879.
- Davoli, T., and de Lange, T. (2011). The causes and consequences of polyploidy in normal development and cancer. *Annu Rev Cell Dev Biol* 27, 585–610.
- De Wever, O., and Mareel, M. (2003). Role of tissue stroma in cancer cell invasion. *J Pathol* 200, 429–447.
- Dehal, P., and Boore, J.L. (2005). Two rounds of whole genome duplication in the ancestral vertebrate. *PLoS Biol.* 3, e314.
- DeNicola, G.M., Karreth, F.A., Humpton, T.J., Gopinathan, A., Wei, C., Frese, K., Mangal, D., Yu, K.H., Yeo, C.J., Calhoun, E.S., et al. (2011). Oncogene-induced Nrf2 transcription promotes ROS detoxification and tumorigenesis. *Nature* 475, 106–109.
- Descot, A., Hoffmann, R., Shaposhnikov, D., Reschke, M., Ullrich, A., and Posern, G. (2009). Negative regulation of the EGFR-MAPK cascade by actin-MAL-mediated Mig6/Errfi-1 induction. *Mol Cell* 35, 291–304.
- Dewhurst, S.M., McGranahan, N., Burrell, R.A., Rowan, A.J., Grönroos, E., Endesfelder, D., Joshi, T., Mouradov, D., Gibbs, P., Ward, R.L., et al. (2014). Tolerance of whole-genome doubling propagates chromosomal instability and accelerates cancer genome evolution. *Cancer Discov* 4, 175–185.
- Dikovskaya, D., Schiffmann, D., Newton, I.P., Oakley, A., Kroboth, K., Sansom, O., Jamieson, T.J., Meniel, V., Clarke, A.R., and Näthke, I.S. (2007). Loss of APC induces polyploidy as a result of a combination of defects in mitosis and apoptosis. *J Cell Biol* 176, 183–195.
- Dimitrov, D.S. (2004). Virus entry: molecular mechanisms and biomedical applications. *Nat Rev Micro* 2, 109–122.
- Doble, B.W., Patel, S., Wood, G.A., Kockeritz, L.K., and Woodgett, J.R. (2007). Functional redundancy of GSK-3alpha and GSK-3beta in Wnt/beta-catenin signaling shown by using an allelic series of embryonic stem cell lines. *Dev Cell* 12, 957–971.
- Dubois, F., Vandermoere, F., Gernez, A., Murphy, J., Toth, R., Chen, S., Geraghty, K.M., Morrice, N.A., and MacKintosh, C. (2009). Differential 14-3-3 affinity capture reveals new downstream targets of phosphatidylinositol 3-kinase signaling. *Mol. Cell Proteomics* 8, 2487–2499.
- Duelli, D.M., and Lazebnik, Y. (2007). Cell-to-cell fusion as a link between viruses and cancer. *Nat Rev Cancer* 7, 968–976.
- Duelli, D.M., Hearn, S., Myers, M.P., and Lazebnik, Y. (2005). A primate virus generates transformed human cells by fusion. *J Cell Biol* 171, 493–503.
-

5. REFERENCES

- Duelli, D.M., Padilla-Nash, H.M., Berman, D., Murphy, K.M., Ried, T., and Lazebnik, Y. (2007). A virus causes cancer by inducing massive chromosomal instability through cell fusion. *Curr Biol* 17, 431–437.
- Elhajouji, A., Cunha, M., and Kirsch-Volders, M. (1998). Spindle poisons can induce polyploidy by mitotic slippage and micronucleate mononucleates in the cytokinesis-block assay. *Mutagenesis* 13, 193–198.
- Fawdar, S., Trotter, E.W., Li, Y., Stephenson, N.L., Hanke, F., Marusiak, A.A., Edwards, Z.C., Ientile, S., Waszkowycz, B., Miller, C.J., et al. (2013). Targeted genetic dependency screen facilitates identification of actionable mutations in FGFR4, MAP3K9, and PAK5 in lung cancer. *Proc Natl Acad Sci USA* 110, 12426–12431.
- Fernandez, P., Maier, M., Lindauer, M., Kuffer, C., Storchova, Z., and Bausch, A.R. (2011). Mitotic spindle orients perpendicular to the forces imposed by dynamic shear. *PLoS ONE* 6, e28965.
- Fleiss, J.L. (2011). Reliability of Measurement. In *Onlinelibrary.Wiley.com*, (Hoboken, NJ, USA: John Wiley & Sons, Inc.), pp. 1–32.
- Foley, E.A., and Kapoor, T.M. (2013). Microtubule attachment and spindle assembly checkpoint signalling at the kinetochore. *Nat Rev Mol Cell Biol* 14, 25–37.
- Fujiwara, T., Bandi, M., Nitta, M., Ivanova, E.V., Bronson, R.T., and Pellman, D. (2005). Cytokinesis failure generating tetraploids promotes tumorigenesis in p53-null cells. *Nature* 437, 1043–1047.
- Galipeau, P.C., Cowan, D.S., Sanchez, C.A., Barrett, M.T., Emond, M.J., Levine, D.S., Rabinovitch, P.S., and Reid, B.J. (1996). 17p (p53) allelic losses, 4N (G2/tetraploid) populations, and progression to aneuploidy in Barrett's esophagus. *Proc Natl Acad Sci USA* 93, 7081–7084.
- Ganem, N.J., and Pellman, D. (2007). Limiting the proliferation of polyploid cells. *Cell* 131, 437–440.
- Ganem, N.J., Godinho, S.A., and Pellman, D. (2009). A mechanism linking extra centrosomes to chromosomal instability. *Nature* 460, 278–282.
- Ganem, N.J., Storchova, Z., and Pellman, D. (2007). Tetraploidy, aneuploidy and cancer. *Curr Opin Genet Dev* 17, 157–162.
- Gao, J., Aksoy, B.A., Dogrusoz, U., Dresdner, G., Gross, B., Sumer, S.O., Sun, Y., Jacobsen, A., Sinha, R., Larsson, E., et al. (2013). Integrative Analysis of Complex Cancer Genomics and Clinical Profiles Using the cBioPortal. *Science Signaling* 6, p11–p11.
- Giaever, G., Chu, A.M., Ni, L., Connelly, C., Riles, L., Véronneau, S., Dow, S., Lucau-Danila, A., Anderson, K., André, B., et al. (2002). Functional profiling of the *Saccharomyces cerevisiae* genome. *Nature* 418, 387–391.
-

5. REFERENCES

- Goktug, A.N., Chai, S.C., and Chen, T. (2013). Data Analysis Approaches in High Throughput Screening. In Intechopen.com, (Drug Discovery).
- Gibbon, P., Lyons, R., Laflin, P., Bradley, J., Chambers, C., Williams, B.S., Keighley, W., and Sewing, A. (2005). Evaluating real-life high-throughput screening data. *J Biomol Screen* 10, 99–107.
- Guerrero, A.A., Gamero, M.C., Trachana, V., Futterer, A., Pacios-Bras, C., Díaz-Concha, N.P., Cigudosa, J.C., Martinez-A, C., and van Wely, K.H.M. (2010). Centromere-localized breaks indicate the generation of DNA damage by the mitotic spindle. *Proc Natl Acad Sci USA* 107, 4159–4164.
- Ha, G.-H., Baek, K.-H., Kim, H.-S., Jeong, S.-J., Kim, C.-M., McKeon, F., and Lee, C.-W. (2007). p53 activation in response to mitotic spindle damage requires signaling via BubR1-mediated phosphorylation. *Cancer Res* 67, 7155–7164.
- Hanahan, D., and Weinberg, R.A. (2011). Hallmarks of cancer: the next generation. *Cell* 144, 646–674.
- Hart, M., Concordet, J.P., Lassot, I., Albert, I., del los Santos, R., Durand, H., Perret, C., Rubinfeld, B., Margottin, F., Benarous, R., et al. (1999). The F-box protein beta-TrCP associates with phosphorylated beta-catenin and regulates its activity in the cell. *Curr Biol* 9, 207–210.
- He, T. (1998). Identification of c-MYC as a Target of the APC Pathway. *Science* 281, 1509–1512.
- Hoffman, G.R., Moerke, N.J., Hsia, M., Shamu, C.E., and Blenis, J. (2010). A high-throughput, cell-based screening method for siRNA and small molecule inhibitors of mTORC1 signaling using the In Cell Western technique. *Assay and Drug Development Technologies* 8, 186–199.
- Hu, L., Plafker, K., Vorozhko, V., Zuna, R.E., Hanigan, M.H., Gorbsky, G.J., Plafker, S.M., Angeletti, P.C., and Ceresa, B.P. (2009). Human papillomavirus 16 E5 induces bi-nucleated cell formation by cell-cell fusion. *Virology* 384, 125–134.
- Huang, D.W., Sherman, B.T., and Lempicki, R.A. (2009a). Bioinformatics enrichment tools: paths toward the comprehensive functional analysis of large gene lists. *Nucleic Acids Res* 37, 1–13.
- Huang, D.W., Sherman, B.T., and Lempicki, R.A. (2009b). Systematic and integrative analysis of large gene lists using DAVID bioinformatics resources. *Nat Protoc* 4, 44–57.
- Huang, H., and He, X. (2008). Wnt/beta-catenin signaling: new (and old) players and new insights. *Curr Opin Cell Biol* 20, 119–125.
- Janssen, A., van der Burg, M., Szuhai, K., Kops, G.J.P.L., and Medema, R.H. (2011). Chromosome segregation errors as a cause of DNA damage and structural chromosome aberrations. *Science* 333, 1895–1898.
-

5. REFERENCES

- Jeganathan, K.B., Malureanu, L., Baker, D.J., Abraham, S.C., and van Deursen, J.M. (2007). Bub1 mediates cell death in response to chromosome missegregation and acts to suppress spontaneous tumorigenesis. *J Cell Biol* 179, 255–267.
- Johnson, L.M., Snyder, M., Chang, L.M., Davis, R.W., and Campbell, J.L. (1985). Isolation of the gene encoding yeast DNA polymerase I. *Cell* 43, 369–377.
- Jones, R.M., Mortusewicz, O., Afzal, I., Lorvellec, M., García, P., Helleday, T., and Petermann, E. (2013). Increased replication initiation and conflicts with transcription underlie Cyclin E-induced replication stress. *Oncogene* 32, 3744–3753.
- JunGang, Z., Jun, T., WanFu, M., and KaiMing, R. (2012). FBXW7-mediated degradation of CCDC6 is impaired by ATM during DNA damage response in lung cancer cells. *FEBS Lett.* 586, 4257–4263.
- Kasahara, M. (2007). The 2R hypothesis: an update. *Curr. Opin. Immunol.* 19, 547–552.
- Katayama, H., Brinkley, W.R., and Sen, S. (2003). The Aurora kinases: role in cell transformation and tumorigenesis. *Cancer Metastasis Rev* 22, 451–464.
- Kim, I., Rodriguez-Enriquez, S., and Lemasters, J.J. (2007). Selective degradation of mitochondria by mitophagy. *Archives of Biochemistry and Biophysics* 462, 245–253.
- Kimura, Y., Morita, T., Hayashi, K., Miki, T., and Sobue, K. (2010). Myocardin functions as an effective inducer of growth arrest and differentiation in human uterine leiomyosarcoma cells. *Cancer Res* 70, 501–511.
- Kinzler, K.W., and Vogelstein, B. (1996). Lessons from hereditary colorectal cancer. *Cell* 87, 159–170.
- Kittler, R., Pelletier, L., Heninger, A.-K., Slabicki, M., Theis, M., Miroslaw, L., Poser, I., Lawo, S., Grabner, H., Kozak, K., et al. (2007). Genome-scale RNAi profiling of cell division in human tissue culture cells. *Nat Cell Biol* 9, 1401–1412.
- Klein, E.A., and Assoian, R.K. (2008). Transcriptional regulation of the cyclin D1 gene at a glance. *J Cell Sci* 121, 3853–3857.
- Kongara, S., and Karantza, V. (2012). The interplay between autophagy and ROS in tumorigenesis. *Front Oncol* 2, 171.
- Kongara, S., Kravchuk, O., Teplova, I., Lozy, F., Schulte, J., Moore, D., Barnard, N., Neumann, C.A., White, E., and Karantza, V. (2010). Autophagy regulates keratin 8 homeostasis in mammary epithelial cells and in breast tumors. *Mol Cancer Res* 8, 873–884.
- Kozik, P., Hodson, N.A., Sahlender, D.A., Simecek, N., Soromani, C., Wu, J., Collinson, L.M., and Robinson, M.S. (2012). A human genome-wide screen for regulators of clathrin-coated vesicle formation reveals an unexpected role for the V-ATPase. *Nat Cell Biol.*
-

5. REFERENCES

- Krastev, D.B., Slabicki, M., Paszkowski-Rogacz, M., Hubner, N.C., Junqueira, M., Shevchenko, A., Mann, M., Neugebauer, K.M., and Buchholz, F. (2011). A systematic RNAi synthetic interaction screen reveals a link between p53 and snoRNP assembly. *Nat Cell Biol*.
- Kuffer, C., Kuznetsova, A.Y., and Storchova, Z. (2013). Abnormal mitosis triggers p53-dependent cell cycle arrest in human tetraploid cells. *Chromosoma* 122, 305–318.
- Kwon, M., Godinho, S.A., Chandhok, N.S., Ganem, N.J., Azioune, A., Thery, M., and Pellman, D. (2008). Mechanisms to suppress multipolar divisions in cancer cells with extra centrosomes. *Genes Dev* 22, 2189–2203.
- Lanni, J.S., and Jacks, T. (1998). Characterization of the p53-dependent postmitotic checkpoint following spindle disruption. *Mol Cell Biol* 18, 1055–1064.
- Lara-Gonzalez, P., Westhorpe, F.G., and Taylor, S.S. (2012). The spindle assembly checkpoint. *Curr Biol* 22, R966–R980.
- Laronga, C., Yang, H.Y., Neal, C., and Lee, M.H. (2000). Association of the cyclin-dependent kinases and 14-3-3 sigma negatively regulates cell cycle progression. *J. Biol. Chem.* 275, 23106–23112.
- Lee, A.J.X., Endesfelder, D., Rowan, A.J., Walther, A., Birkbak, N.J., Futreal, P.A., Downward, J., Szallasi, Z., Tomlinson, I.P.M., Howell, M., et al. (2011). Chromosomal instability confers intrinsic multidrug resistance. *Cancer Res* 71, 1858–1870.
- Lee, H.O., Davidson, J.M., and Duronio, R.J. (2009). Endoreplication: polyploidy with purpose. *Genes Dev* 23, 2461–2477.
- Leland H Hartwell, R.K.M.J.C.M.C. (1973). Genetic Control of the Cell Division Cycle in Yeast: V. Genetic Analysis of cdc Mutants. *Genetics* 74, 267–286.
- Lemasters, J.J. (2005). Selective mitochondrial autophagy, or mitophagy, as a targeted defense against oxidative stress, mitochondrial dysfunction, and aging. *Rejuvenation Res* 8, 3–5.
- Levayer, R., and Moreno, E. (2013). Mechanisms of cell competition: themes and variations. *J Cell Biol* 200, 689–698.
- Li, B., Kuriyama, S., Moreno, M., and Mayor, R. (2009). The posteriorizing gene Gbx2 is a direct target of Wnt signalling and the earliest factor in neural crest induction. *Development* 136, 3267–3278.
- Li, M., Fang, X., Baker, D.J., Guo, L., Gao, X., Wei, Z., Han, S., van Deursen, J.M., and Zhang, P. (2010). The ATM-p53 pathway suppresses aneuploidy-induced tumorigenesis. *107*, 14188–14193.
- Liu, C., Kato, Y., Zhang, Z., Do, V.M., Yankner, B.A., and He, X. (1999). beta-Trcp couples beta-catenin phosphorylation-degradation and regulates Xenopus axis formation. *Proc Natl Acad Sci USA* 96, 6273–6278.
-

5. REFERENCES

- Loeb, L.A., and Monnat, R.J. (2008). DNA polymerases and human disease. *Nat Rev Genet* 9, 594–604.
- Lv, L., Zhang, T., Yi, Q., Huang, Y., Wang, Z., Hou, H., Zhang, H., Zheng, W., Hao, Q., Guo, Z., et al. (2012). Tetraploid cells from cytokinesis failure induce aneuploidy and spontaneous transformation of mouse ovarian surface epithelial cells. *Cc* 11, 2864–2875.
- MacDonald, B.T., Tamai, K., and He, X. (2009). Wnt/beta-catenin signaling: components, mechanisms, and diseases. *Dev Cell* 17, 9–26.
- Maley, C.C. (2007). Multistage carcinogenesis in Barrett's esophagus. *Cancer Lett* 245, 22–32.
- Mann, B., Gelos, M., Siedow, A., Hanski, M.L., Gratchev, A., Ilyas, M., Bodmer, W.F., Moyer, M.P., Riecken, E.O., Buhr, H.J., et al. (1999). Target genes of beta-catenin-T cell-factor/lymphoid-enhancer-factor signaling in human colorectal carcinomas. *Proc Natl Acad Sci USA* 96, 1603–1608.
- Marsh, M., and Helenius, A. (2006). Virus entry: open sesame. *Cell* 124, 729–740.
- Mathew, R., Karp, C.M., Beaudoin, B., Vuong, N., Chen, G., Chen, H.-Y., Bray, K., Reddy, A., Bhanot, G., Gelinas, C., et al. (2009). Autophagy suppresses tumorigenesis through elimination of p62. *Cell* 137, 1062–1075.
- Meraldi, P., Honda, R., and Nigg, E.A. (2002). Aurora-A overexpression reveals tetraploidization as a major route to centrosome amplification in p53^{-/-} cells. *Embo J* 21, 483–492.
- Miano, J.M., Long, X., and Fujiwara, K. (2007). Serum response factor: master regulator of the actin cytoskeleton and contractile apparatus. *Am. J. Physiol., Cell Physiol.* 292, C70–C81.
- Micale, M.A., Schran, D., Emch, S., Kurczynski, T.W., Rahman, N., and Van Dyke, D.L. (2007). Mosaic variegated aneuploidy without microcephaly: implications for cytogenetic diagnosis. *Am J Med Genet A* 143A, 1890–1893.
- Morgan, D. (2007). *The Cell Cycle* (New Science Press).
- Mullins, J.M., and Biesele, J.J. (1977). Terminal phase of cytokinesis in D-98s cells. *J Cell Biol* 73, 672–684.
- Musacchio, A., and Salmon, E.D. (2007). The spindle-assembly checkpoint in space and time. *Nat Rev Mol Cell Biol* 8, 379–393.
- Nakada, S., Chen, G.I., Gingras, A.-C., and Durocher, D. (2008). PP4 is a gamma H2AX phosphatase required for recovery from the DNA damage checkpoint. *EMBO Rep* 9, 1019–1026.
- Neumann, B., Held, M., Liebel, U., Erfle, H., Rogers, P., Pepperkok, R., and Ellenberg, J. (2006). High-throughput RNAi screening by time-lapse imaging of live human cells. *Nat Methods* 3, 385–390.
-

5. REFERENCES

- Neumann, B., Walter, T., Hériché, J.-K., Bulkescher, J., Erfle, H., Conrad, C., Rogers, P., Poser, I., Held, M., Liebel, U., et al. (2010). Phenotypic profiling of the human genome by time-lapse microscopy reveals cell division genes. *Nature* *464*, 721–727.
- Nezi, L., and Musacchio, A. (2009). Sister chromatid tension and the spindle assembly checkpoint. *Curr Opin Cell Biol* *21*, 785–795.
- Novak, B., Sible, J.C., and Tyson, J.J. (2001). Checkpoints in the Cell Cycle (Chichester, UK: John Wiley & Sons, Ltd).
- Ohno, S. (1970). Evolution by gene duplication (Berlin, New York : Springer Verlag).
- Olaharski, A.J., Sotelo, R., Solorza-Luna, G., Gonsebatt, M.E., Guzman, P., Mohar, A., and Eastmond, D.A. (2006). Tetraploidy and chromosomal instability are early events during cervical carcinogenesis. *Carcinogenesis* *27*, 337–343.
- Ornitz, D.M., Hammer, R.E., Messing, A., Palmiter, R.D., and Brinster, R.L. (1987). Pancreatic neoplasia induced by SV40 T-antigen expression in acinar cells of transgenic mice. *Science* *238*, 188–193.
- Pearson, G., Robinson, F., Beers Gibson, T., Xu, B.E., Karandikar, M., Berman, K., and Cobb, M.H. (2001). Mitogen-activated protein (MAP) kinase pathways: regulation and physiological functions. *Endocr. Rev.* *22*, 153–183.
- Pelicano, H., Carney, D., and Huang, P. (2004). ROS stress in cancer cells and therapeutic implications. *Drug Resist. Updat.* *7*, 97–110.
- Pellman, D. (2007). Cell biology: aneuploidy and cancer. *Nature* *446*, 38–39.
- Perera, R.M., and Bardeesy, N. (2011). Cancer: when antioxidants are bad. *Nature* *475*, 43–44.
- Polakis, P. (1997). The adenomatous polyposis coli (APC) tumor suppressor. *Biochim Biophys Acta* *1332*, F127–F147.
- Polo, S.E., and Jackson, S.P. (2011). Dynamics of DNA damage response proteins at DNA breaks: a focus on protein modifications. *Genes Dev* *25*, 409–433.
- Posern, G., and Treisman, R. (2006). Actin' together: serum response factor, its cofactors and the link to signal transduction. *Trends Cell Biol* *16*, 588–596.
- Putnam, N.H., Butts, T., Ferrier, D.E.K., Furlong, R.F., Hellsten, U., Kawashima, T., Robinson-Rechavi, M., Shoguchi, E., Terry, A., Yu, J.-K., et al. (2008). The amphioxus genome and the evolution of the chordate karyotype. *Nature* *453*, 1064–1071.
- Quignon, F., Rozier, L., Lachages, A.-M., Bieth, A., Simili, M., and Debatisse, M. (2007). Sustained mitotic block elicits DNA breaks: one-step alteration of ploidy and chromosome integrity in mammalian cells. *Oncogene* *26*, 165–172.

5. REFERENCES

R Core Team (2012). R: A language and environment for statistical computing. R Foundation for Statistical Computing, Vienna, Austria. ISBN 3-900051-07-0 Available from <http://www.R-project.org/>.

Rago, F., and Cheeseman, I.M. (2013). Review series: The functions and consequences of force at kinetochores. *J Cell Biol* 200, 557–565.

Ramanan, V.K., Shen, L., Moore, J.H., and Saykin, A.J. (2012). Pathway analysis of genomic data: concepts, methods, and prospects for future development. *Trends Genet.* 28, 323–332.

Rawlings, J.S., Rosler, K.M., and Harrison, D.A. (2004). The JAK/STAT signaling pathway. *J Cell Sci* 117, 1281–1283.

Reverte, C.G., Benware, A., Jones, C.W., and LaFlamme, S.E. (2006). Perturbing integrin function inhibits microtubule growth from centrosomes, spindle assembly, and cytokinesis. *J Cell Biol* 174, 491–497.

RStudio (2013). RStudio: Integrated development environment for R (Version 0.97.258). Boston, MA. Available from <http://www.rstudio.org/>

Ruggero, D., and Pandolfi, P.P. (2003). Does the ribosome translate cancer? *Nat Rev Cancer* 3, 179–192.

Sakaue-Sawano, A., Kurokawa, H., Morimura, T., Hanyu, A., Hama, H., Osawa, H., Kashiwagi, S., Fukami, K., Miyata, T., Miyoshi, H., et al. (2008). Visualizing Spatiotemporal Dynamics of Multicellular Cell-Cycle Progression. *Cell* 132, 487–498.

Satoh, S., Daigo, Y., Furukawa, Y., Kato, T., Miwa, N., Nishiwaki, T., Kawasoe, T., Ishiguro, H., Fujita, M., Tokino, T., et al. (2000). AXIN1 mutations in hepatocellular carcinomas, and growth suppression in cancer cells by virus-mediated transfer of AXIN1. *Nat Genet* 24, 245–250.

Schvartzman, J.-M., Duijf, P.H.G., Sotillo, R., Coker, C., and Benezra, R. (2011). Mad2 Is a Critical Mediator of the Chromosome Instability Observed upon Rb and p53 Pathway Inhibition. *Cancer Cell* 19, 701–714.

Shackney, S.E., Smith, C.A., Miller, B.W., Burholt, D.R., Murtha, K., Giles, H.R., Ketterer, D.M., and Pollice, A.A. (1989). Model for the genetic evolution of human solid tumors. *Cancer Res* 49, 3344–3354.

Shaposhnikov, D., Kuffer, C., Storchova, Z., and Posern, G. (2013). Myocardin related transcription factors are required for coordinated cell cycle progression. *Cc* 12, 1762–1772.

Shen, M., Schmitt, S., Buac, D., and Dou, Q.P. (2013). Targeting the ubiquitin-proteasome system for cancer therapy. *Expert Opin. Ther. Targets* 17, 1091–1108.

Shi, Q., and King, R.W. (2005). Chromosome nondisjunction yields tetraploid rather than aneuploid cells in human cell lines. *Nature* 437, 1038–1042.

5. REFERENCES

- Shibutani, S., Takeshita, M., and Grollman, A.P. (1991). Insertion of specific bases during DNA synthesis past the oxidation-damaged base 8-oxodG. *Nature* **349**, 431–434.
- Shiloh, Y., and Ziv, Y. (2013). The ATM protein kinase: regulating the cellular response to genotoxic stress, and more. *Nat Rev Mol Cell Biol* **14**, 197–210.
- Shin, H.J., Baek, K.H., Jeon, A.H., Park, M.T., Lee, S.J., Kang, C.M., Lee, H.S., Yoo, S.H., Chung, D.H., Sung, Y.C., et al. (2003). Dual roles of human BubR1, a mitotic checkpoint kinase, in the monitoring of chromosomal instability. *Cancer Cell* **4**, 483–497.
- Shtutman, M., Zhurinsky, J., Simcha, I., Albanese, C., D'Amico, M., Pestell, R., and Ben-Ze'ev, A. (1999). The cyclin D1 gene is a target of the beta-catenin/LEF-1 pathway. *Proc Natl Acad Sci USA* **96**, 5522–5527.
- Sotillo, R., Hernando, E., Díaz-Rodríguez, E., Teruya-Feldstein, J., Cordon-Cardo, C., Lowe, S.W., and Benezra, R. (2007). Mad2 overexpression promotes aneuploidy and tumorigenesis in mice. *Cancer Cell* **11**, 9–23.
- Stark, G.R., and Taylor, W.R. (2006). Control of the G2/M transition. *Mol. Biotechnol.* **32**, 227–248.
- Stingele, S., Stoehr, G., Peplowska, K., Cox, J., Mann, M., and Storchova, Z. (2012). Global analysis of genome, transcriptome and proteome reveals the response to aneuploidy in human cells. *Mol. Syst. Biol.* **8**, 608.
- Stolz, A., Ertych, N., Kienitz, A., Vogel, C., Schneider, V., Fritz, B., Jacob, R., Dittmar, G., Weichert, W., Petersen, I., et al. (2010). The CHK2-BRCA1 tumour suppressor pathway ensures chromosomal stability in human somatic cells. *Nat Cell Biol.*
- Storchova, Z., and Kuffer, C. (2008). The consequences of tetraploidy and aneuploidy. *J Cell Sci* **121**, 3859–3866.
- Storchova, Z., and Pellman, D. (2004). From polyploidy to aneuploidy, genome instability and cancer. *Nat Rev Mol Cell Biol* **5**, 45–54.
- Symington, L.S., and Gautier, J. (2011). Double-strand break end resection and repair pathway choice. *Annu Rev Genet* **45**, 247–271.
- Tang, R.-H., Zheng, X.-L., Callis, T.E., Stansfield, W.E., He, J., Baldwin, A.S., Wang, D.-Z., and Selzman, C.H. (2008). Myocardin inhibits cellular proliferation by inhibiting NF-kappaB(p65)-dependent cell cycle progression. *Proc Natl Acad Sci USA* **105**, 3362–3367.
- Tetsu, O., and McCormick, F. (1999). Beta-catenin regulates expression of cyclin D1 in colon carcinoma cells. *Nature* **398**, 422–426.
- Thanasopoulou, A., Stravopodis, D.J., Dimas, K.S., Schwaller, J., and Anastasiadou, E. (2012). Loss of CCDC6 affects cell cycle through impaired intra-S-phase
-

5. REFERENCES

checkpoint control. *PLoS ONE* 7, e31007.

Theis, M., and Buchholz, F. (2011). High-throughput RNAi screening in mammalian cells with esiRNAs. *Methods* 53, 424–429.

Theis, M., Slabicki, M., Junqueira, M., Paszkowski-Rogacz, M., Sontheimer, J., Kittler, R., Heninger, A.-K., Glatter, T., Kruusmaa, K., Poser, I., et al. (2009). Comparative profiling identifies C13orf3 as a component of the Ska complex required for mammalian cell division. *Embo J* 28, 1453–1465.

Thompson, S.L., and Compton, D.A. (2010). Proliferation of aneuploid human cells is limited by a p53-dependent mechanism. *J Cell Biol* 188, 369–381.

Trotter, J. (2007). Alternatives to log-scale data display. *Curr Protoc Cytom Chapter 10*, Unit10.16.

Truman, A.W., Kitazono, A.A., Fitz Gerald, J.N., and Kron, S.J. (2001). *Cell Cycle: Regulation by Cyclins* (Chichester, UK: John Wiley & Sons, Ltd).

Uetake, Y., and Sluder, G. (2004). Cell cycle progression after cleavage failure: mammalian somatic cells do not possess a “tetraploidy checkpoint.” *J Cell Biol* 165, 609–615.

Uetake, Y., and Sluder, G. (2010). Prolonged Prometaphase Blocks Daughter Cell Proliferation Despite Normal Completion of Mitosis. *Current Biology* 20, 1666–1671.

Vainio, P., Mpindi, J.-P., Kohonen, P., Fey, V., Mirtti, T., Alanen, K.A., Perälä, M., Kallioniemi, O., and Iljin, K. (2012). High-throughput transcriptomic and RNAi analysis identifies AIM1, ERGIC1, TMED3 and TPX2 as potential drug targets in prostate cancer. *PLoS ONE* 7, e39801.

van de Wetering, M., Sancho, E., Verweij, C., de Lau, W., Oving, I., Hurlstone, A., van der Horn, K., Batlle, E., Coudreuse, D., Haramis, A.P., et al. (2002). The beta-catenin/TCF-4 complex imposes a crypt progenitor phenotype on colorectal cancer cells. *Cell* 111, 241–250.

van Iersel, M.P., Kelder, T., Pico, A.R., Hanspers, K., Coort, S., Conklin, B.R., and Evelo, C. (2008). Presenting and exploring biological pathways with PathVisio. *BMC Bioinformatics* 9, 399.

Veitia, R.A. (2010). A generalized model of gene dosage and dominant negative effects in macromolecular complexes. *Faseb J.* 24, 994–1002.

Vermeulen, K., Van Bockstaele, D.R., and Berneman, Z.N. (2003). The cell cycle: a review of regulation, deregulation and therapeutic targets in cancer. *Cell Prolif.* 36, 131–149.

Vink, M., Simonetta, M., Transidico, P., Ferrari, K., Mapelli, M., De Antoni, A., Massimiliano, L., Ciliberto, A., Faretta, M., Salmon, E.D., et al. (2006). In vitro FRAP identifies the minimal requirements for Mad2 kinetochore dynamics. *Curr Biol* 16, 755–766.

5. REFERENCES

- Vitale, I., Galluzzi, L., Vivet, S., Nanty, L., Dessen, P., Senovilla, L., Olaussen, K.A., Lazar, V., Prudhomme, M., Golsteyn, R.M., et al. (2007). Inhibition of Chk1 Kills Tetraploid Tumor Cells through a p53-Dependent Pathway. *PLoS ONE* 2, e1337.
- Wagstaff, L., Kolahgar, G., and Piddini, E. (2013). Competitive cell interactions in cancer: a cellular tug of war. *Trends Cell Biol* 23, 160–167.
- Wang, X., Zhou, Y.-X., Qiao, W., Tominaga, Y., Ouchi, M., Ouchi, T., and Deng, C.-X. (2006). Overexpression of aurora kinase A in mouse mammary epithelium induces genetic instability preceding mammary tumor formation. *Oncogene* 25, 7148–7158.
- Wickham, H. (2009). *ggplot2: elegant graphics for data analysis* (Springer New York).
- Williams, B.R., Prabhu, V.R., Hunter, K.E., Glazier, C.M., Whittaker, C.A., Housman, D.E., and Amon, A. (2008). Aneuploidy affects proliferation and spontaneous immortalization in mammalian cells. *Science* 322, 703–709.
- Wong, C., and Stearns, T. (2005). Mammalian cells lack checkpoints for tetraploidy, aberrant centrosome number, and cytokinesis failure. *BMC Cell Biol* 6, 6.
- Yang, Z., Loncarek, J., Khodjakov, A., and Rieder, C.L. (2008). Extra centrosomes and/or chromosomes prolong mitosis in human cells. *Nat Cell Biol* 10, 748–751.
- Youle, R.J., and Narendra, D.P. (2011). Mechanisms of mitophagy. *Nat Rev Mol Cell Biol* 12, 9–14.
- Zack, T.I., Schumacher, S.E., Carter, S.L., Cherniack, A.D., Saksena, G., Tabak, B., Lawrence, M.S., Zhang, C.-Z., Wala, J., Mermel, C.H., et al. (2013). Pan-cancer patterns of somatic copy number alteration. *Nat Genet* 45, 1134–1140.
- Zhang, X.D. (2011). *Optimal High-Throughput Screening* (Cambridge Univ Pr).

V. ACKNOWLEDGEMENT

I am very much obliged to Dr. Zuzana Stochová for providing the possibility to work in her lab on this interesting topic and her continuous support.

I would like to thank Prof. Stefan Jentsch for the hospitality provided by his department and for taking over the official supervision.

I am grateful to Prof. Angelika Böttger for co-referring this thesis. I am indebted to Prof. Peter Becker and Prof. Martin Parniske for being in my thesis committee and Prof. Babara Conradt and Prof. John Parsch for careful reading and evaluation of my dissertation.

I would like to thank my collaboration partners Prof. Frank Buchholz, Dr. Dragomir Krastev and Dr. Mirko Theis previously at MPI-CBG in Dresden. Further, Prof. Dr. Andreas Bausch and Dr. Pablo Fernandez from the department biophysics of the Technical University Munich as well as Prof. Guido Posern and Dr. Dmitry Shaposhnikov from the Institute for Physiological Chemistry at the Martin-Luther-University in Halle (Saale).

Also, I am grateful to Prof. Reinhard Fässler for the access to his flow cytometry facility and Dr. Raphael Ruppert for providing constant support.

Special thanks go to Dr. Thomas Gaintanos and Dr. Steven Bergink for helpful discussion as well all given hints.

I am very thankful to Jochen Rech for the great introduction into automated liquid handling and his continuous support.

I am indebted to Susanne Gutmann, Aline de Campos Sparr, Sandra Kurz and Daniela Fellner for technical assistance.

Finally, I thank my lab colleagues Dr. Silvia Stingele, Dr. Anastasia Kuznetsova, Dr. Carolina Peplowska, Krishna Sreenivasan, Andreas Wallek, Verena Passerini, Neyson Donnelly for great lab atmosphere.